

## Three-dimensional simulations of long-lived tracers using winds from MACCM2

D. W. Waugh,<sup>1</sup> T. M. Hall,<sup>1</sup> W. J. Randel,<sup>2</sup> P. J. Rasch,<sup>2</sup> B. A. Boville,<sup>2</sup> K. A. Boering,<sup>3</sup> S. C. Wofsy,<sup>3</sup> B. C. Daube,<sup>3</sup> J. W. Elkins,<sup>4</sup> D. W. Fahey,<sup>5</sup> G. S. Dutton,<sup>4,6</sup> C. M. Volk,<sup>4,6</sup> and P. F. Vohralik.<sup>7</sup>

**Abstract.** Three-dimensional simulations of the stratospheric constituents CH<sub>4</sub>, N<sub>2</sub>O, O<sub>3</sub>, SF<sub>6</sub>, and CO<sub>2</sub> over an annual cycle have been performed using a semi-Lagrangian chemical transport model [*Rasch and Williamson, 1990; Rasch et al., 1994*] driven by archived wind data from the Middle Atmosphere version of the National Center for Atmospheric Research Community Climate Model version 2 (MACCM2) general circulation model. The constituents undergo chemical production and loss at rates calculated by two-dimensional photochemical models. We compare these “off-line” simulations of CH<sub>4</sub> and N<sub>2</sub>O with “on-line” simulations in which the trace constituent distributions are computed interactively within the MACCM2 general circulation model and find good agreement even when daily averaged wind data and no subgrid scale parameterized mixing are used in the off-line simulations. We also compare the model simulations to satellite, aircraft, and balloon measurements. In most regions and seasons, the zonally averaged model CH<sub>4</sub>, N<sub>2</sub>O, and O<sub>3</sub> fields agree well with observations. Notable discrepancies are (1) a lack of a “double peak” structure in the zonally averaged mixing ratios of model CH<sub>4</sub> and N<sub>2</sub>O at equinox, (2) an overall underestimate of CH<sub>4</sub> and N<sub>2</sub>O in the upper stratosphere, and (3) an underestimate of the height of the mixing ratio peak in O<sub>3</sub>, particularly at high latitudes. We find good agreement between modeled CO<sub>2</sub> and SF<sub>6</sub> and recent aircraft observations in the lower stratosphere, and balloon measurements in the lower and middle stratosphere. From the SF<sub>6</sub> distribution we determine the mean age of air in the model stratosphere, with values as old as 10 years in the wintertime polar upper stratosphere. In addition, we simulate the annual cycle of CO<sub>2</sub>, a stringent test of model transport, which supplements the mean age. We obtain good agreement with aircraft measurements in phase and magnitude at the tropical tropopause, and the vertical profiles of CO<sub>2</sub> are similar to those observed. However, the amplitude of the cycle attenuates too rapidly with height in the model stratosphere, suggesting the influence of midlatitude air and/or the vertical diffusion are too large in the model tropics.

<sup>1</sup>Cooperative Research Centre for Southern Hemisphere Meteorology, Monash University, Clayton, Victoria, Australia.

<sup>2</sup>National Center for Atmospheric Research, Boulder, Colorado.

<sup>3</sup>Division of Applied Sciences and Department of Earth and Planetary Sciences, Harvard University, Cambridge, Massachusetts.

<sup>4</sup>Climate Monitoring and Diagnostics Laboratory, National Oceanic and Atmospheric Administration, Boulder, Colorado.

<sup>5</sup>Aeronomy Laboratory, National Oceanic and Atmospheric Administration, Boulder, Colorado.

<sup>6</sup>Cooperative Institute for Research in Environmental Sciences, Boulder, Colorado.

<sup>7</sup>Commonwealth Scientific and Industrial Research Organisation, Division of Telecommunications and Industrial Physics, Lindfield, New South Wales, Australia.

Copyright 1997 by the American Geophysical Union.

Paper number 97JD00793.  
0148-0227/97/97JD-00793\$09.00

## 1. Introduction

In recent years researchers have increasingly used three-dimensional models of the stratosphere, and such models will become the tools of choice for predicting human impact on stratospheric composition and climate. Two-dimensional models have been the workhorses over the past two decades for assessing the impact of anthropogenic trace gas releases, such as the effluent of proposed high speed civil aircraft fleets [*Stolarski et al., 1995*]. These models have incorporated increasingly detailed and realistic atmospheric chemistry, simulating the distributions of many interacting constituents. Their zonally averaged representation of transport, however, necessitates a somewhat ad-hoc treatment of dynamical phenomena, such as the isolated winter polar vortex and the “barrier” separating the tropics from the extratropics in the lower stratosphere. These are features crucial for modeling chemically perturbed regions, such as the ozone hole, and predicting the dis-

persal of aircraft emissions. Three-dimensional models naturally represent more completely the array of waves that are a vital part of stratospheric transport. Several stratospheric general circulation models (GCMs) simulate long-lived tracers, such as  $\text{N}_2\text{O}$  and  $\text{CH}_4$ , simultaneously with their computation of stratospheric winds using parameterized chemistry [Mahlman et al., 1986; Strahan and Mahlman, 1994; Randel et al., 1994]. More recently, Rasch et al. [1995] and Eckman et al. [1995] have run multiyear GCM simulations with interacting chemistry, albeit with photochemical quasi-equilibrium assumptions so that not all species need be transported.

However, the computational demands of “on-line” GCM simulations with interacting chemistry make another class of three-dimensional models attractive: “off-line” chemical transport models (CTMs), which do not compute the wind fields but instead accept these data as input from another source. (Hereinafter we use “on-line” to refer to simulations which compute the meteorological fields as well as the tracer fields, and “off-line” to refer to simulations which use prescribed meteorological fields.) CTMs are both an intermediate step toward three-dimensional fully interactive chemical-dynamical models and research tools in their own right. They represent a compromise between the intense computational requirements of multispecies interacting chemistry and fluid dynamics. Although off-line modeling neglects possible feedbacks between chemical evolution and dynamics, the reduction in dynamical computation provides the opportunity for a corresponding increase in chemical computation, allowing the inclusion of a number of chemically interacting constituents. Alternatively, the CTM’s relative computational speed with simple lone tracers is advantageous for performing extensive sensitivity studies and numerical tests of hypothesized transport mechanisms. Compared to zonally averaged models, the transport in the CTM includes the same three-dimensional features of the driving wind data set.

Another advantage of off-line CTMs is the ability to perform simulations using wind data assimilated from observations. In recent years there have been many CTM studies using assimilated data to examine the interaction between transport and chemical processes in the stratosphere [Rood et al., 1990; Rood et al., 1991; Douglass et al., 1993; Lefevre et al., 1994; Chipperfield et al., 1994]. These studies have focused on the wintertime behavior in polar regions, and the simulations were generally for week- to month-long timescales. However, recently, Douglass et al. [1996] modeled ozone over a full year using assimilated winds.

One of the main goals of this study is to determine the degree to which off-line (CTM) simulations approximate on-line (GCM) simulations. In addition to the neglect of chemical-dynamical feedback, off-line simulations have a further level of approximation: the wind data are necessarily archived at a lower time resolu-

tion than the fundamental GCM time step. What price is paid by using averaged or subsampled wind data? Rasch et al. [1994] addressed this question with stratospheric simulations of idealized conserved tracers over week timescales, Rayner and Law [1996] compared on-line and off-line simulations of tropospheric  $\text{CO}_2$ , and P. J. Rasch et al. (Representations of transport, convection and the hydrologic cycle in chemical transport models: Implications for the modeling of short lived and soluble species, submitted to *Journal of Geophysical Research*, 1997; hereinafter referred to as submitted manuscript) examined simulations of short-lived tropospheric tracers. However, to our knowledge, this issue has not been examined for simulations of the annual climatologies of realistic stratospheric trace gases. In this study we address this issue by comparing off-line and on-line simulations of methane ( $\text{CH}_4$ ) and nitrous oxide ( $\text{N}_2\text{O}$ ) over a year.

A second goal is to verify the realism of a suite of modeled three-dimensional tracer distributions over an annual cycle by comparing to satellite, aircraft, and balloon observations. Such verification is a necessary first step before the fields can be used meaningfully for studies of stratospheric transport. As well as  $\text{CH}_4$  and  $\text{N}_2\text{O}$ , we also simulate the annual climatologies of ozone ( $\text{O}_3$ ), sulfur hexafluoride ( $\text{SF}_6$ ), and carbon dioxide ( $\text{CO}_2$ ). To our knowledge, the only previous three-dimensional simulations of stratospheric  $\text{SF}_6$  and  $\text{CO}_2$  are those by [Hall and Prather, 1993; Hall and Prather, 1995] (note that their “ $\text{CO}_2^T$ ” tracer is equivalent to our  $\text{SF}_6$  tracer). We compare our  $\text{SF}_6$  and  $\text{CO}_2$  simulations with the simulations of Hall and Prather, and with recent aircraft measurements in the lower stratosphere [Elkins et al., 1996; Boering et al., 1996] and balloon measurements in lower and middle stratosphere [Harnisch et al., 1996].

The CTM and the details of the simulations performed are described in the following section. In section 3, off-line simulations of  $\text{CH}_4$  are compared to on-line simulations of the same constituent. The simulations of  $\text{CH}_4$ ,  $\text{N}_2\text{O}$ ,  $\text{O}_3$ ,  $\text{SF}_6$ , and  $\text{CO}_2$  are analyzed and compared to observations in section 4. In section 5 we conclude and discuss upcoming applications for the CTM.

## 2. Model and Simulation Descriptions

### 2.1. Model Description

In this study we use the chemical transport model developed at National Center for Atmospheric Research (NCAR) by Rasch and Williamson [1990] and Rasch et al. [1994]. This model uses a semi-Lagrangian transport scheme, which preserves shapes of tracer distributions and minimizes numerical diffusion [Williamson and Rasch, 1989]. The scheme is not implicitly mass conservative, and a “mass fixer” is employed after advection to keep global tracer mass constant (see Appendix of Rasch et al. [1995] for description of the mass fixer used). This transport model has been used, for example, to simulate stratospheric aerosols [Boville

*et al.*, 1991], radioactive isotopes [Rasch *et al.*, 1994], chlorofluorocarbons (CFCs) in the troposphere [Hartley *et al.*, 1994], and stratospheric tracer species [Rasch *et al.*, 1995].

The CTM is driven by wind fields from the Middle Atmosphere version of the NCAR Community Climate Model version 2 (MACCM2) [Boville, 1995]. The MACCM2 simulation has T42 horizontal resolution (128 × 64 longitude by latitude points, giving an approximate horizontal resolution of 2.8°), and there are 44 vertical levels from the surface to  $p \approx 0.01$  hPa (80 km). Of those, 28 are at fixed pressure levels above 16 km; the vertical resolution in the lower stratosphere is approximately 1.4 km. Note that the Rasch-Williamson semi-Lagrangian transport scheme is used in the MACCM2 to transport moisture and tracer constituents.

The climatology of MACCM2 is described by Boville [1995]. The northern stratosphere is realistic, but there are problems in the southern stratosphere. In particular, the magnitude of the southern polar jet is almost twice that observed, and polar temperatures are 30 K to 40 K colder than observed. The MACCM2 simulation produces a semiannual oscillation (SAO) (although the westerly phase is too weak [Sassi *et al.*, 1993]), but there is no quasi-biennial oscillation.

## 2.2. Specifics of the Simulations

In this study we focus on simulations of trace constituent distributions in the upper troposphere and stratosphere. Thus we sacrifice realism below the upper troposphere for the sake of simplicity of simulation. Our approach is to use a simple, in most cases uniform, boundary condition on the tracer mixing ratio in the first three model levels from the surface. At each model time step the mixing ratio is set to this value, which is selected to match observed mean tropospheric abundances. The tracers modeled here have incompletely understood sources and sinks at the surface, and these sources and sinks have high geographic structure. However, the signature in the atmospheric mixing ratio of zonal features in the sources and sinks are attenuated rapidly with height (see, for example, the CO<sub>2</sub> studies of Heimann *et al.* [1989]), so that by the upper troposphere only the zonally averaged latitudinal dependence of the mixing ratio is apparent. Moreover, as most air enters the stratosphere in the tropics, even the latitudinal variation of the surface sources and sinks causes only small uniform offsets in the stratosphere and has little effect on the mixing ratio gradients (see Hall and Plumb [1994] for a discussion of the stratospheric impact of latitudinal shifts in modeled surface source). With the exception of the latitudinally dependent annual cycle forcing of CO<sub>2</sub>, all tracers modeled here have uniform surface boundary conditions.

To model the chemical evolution of the tracers we use “look-up” tables of coefficients of production ( $P$ ), linear loss ( $L$ ), and quadratic loss ( $Q$ ) that are functions

of latitude, height, and month of year. These coefficients have been previously computed by explicit solution of multispecies two-dimensional (2-D) photochemical models. At each CTM time step, the tracer change due to chemical production and loss is determined by using the values read from the tables in the equation

$$\frac{\partial \chi}{\partial t} = P - L\chi - Q\chi^2 \quad (1)$$

where  $\chi$  is the tracer mixing ratio. Such a formulation assumes no interaction among the species modeled in the CTM.

Except when explicitly testing the sensitivity to wind sampling frequency and parameterized mixing (see section 3), we use 24-hourly averaged MACCM2 wind data and include no representation of subgrid scale processes. A 1-hour time step is used for advecting the tracers, and the wind at each time step is determined by linear interpolation from the input wind data. In all simulations 1 year of wind data is used, and thus no interannual variability in the tracer distributions is modeled. We recycle the winds in order to integrate for several years and achieve a “cyclostationary” steady state, that is, a state in which the mixing ratio anywhere in the atmosphere at a particular date is negligibly different from the value at the same location and date 1 year prior. Using as initial conditions on-line tracer distributions from the MACCM2 GCM, a cyclostationary state for CH<sub>4</sub> and N<sub>2</sub>O takes approximately 2 years to achieve (note that the final state, but not the time taken to reach this state, is independent of the initial state). Details relevant to particular species are as follows.

**2.2.1 Methane.** The major source of atmospheric CH<sub>4</sub> is anaerobic microbial activity at the Earth’s surface. CH<sub>4</sub> is long lived in the lower stratosphere, having local chemical lifetimes greater than 10 years below 25 km, decreasing to about 4 months at 40 km [Brasseur and Solomon, 1984], and is removed, primarily by oxidation, above 35 km. This long lifetime makes CH<sub>4</sub> a useful tracer of stratospheric transport. In terms of expression (1),  $P = Q = 0$ , and  $L$  is derived from the photochemical modeling work of Garcia and Solomon [1983]. (We have also performed a simulation using  $L$  derived from the Commonwealth Scientific and Industrial Research Organisation (CSIRO) Division of Telecommunications and Industrial Physics (DTIP) two-dimensional chemical transport model [Stolarski *et al.*, 1995; L. K. Randeniya *et al.* (Impact of heterogeneous BrONO<sub>2</sub> hydrolysis on NO<sub>2</sub> columns at high latitudes in summer and on ozone at middle and high latitudes, submitted to *Journal of Geophysical Research*, 1997; hereinafter referred to as submitted manuscript)], and the resulting CH<sub>4</sub> distribution was very similar.) Although CH<sub>4</sub> has a significant positive tropospheric trend of about 1 % per year, its gradients in the stratosphere are primarily due to the chemical loss aloft. In our simulations we hold the mixing ratios in the first three model levels from the surface at a constant 1700 parts per billion (ppb).

**2.2.2 Nitrous Oxide.** Like  $\text{CH}_4$ ,  $\text{N}_2\text{O}$  has its source at the surface, and is long lived in the lower stratosphere. The sources of  $\text{N}_2\text{O}$  are both anthropogenic and natural (microbial activity in the soil and oceans), and it is destroyed by photolysis and reaction with  $\text{O}(^1\text{D})$  in the upper stratosphere. The local chemical lifetime of  $\text{N}_2\text{O}$  is about 50 years at 25 km in the tropics [Brasseur and Solomon, 1984], decreasing rapidly aloft. The coefficients  $P$  and  $Q$  in (1) are 0, and  $L$  is from Garcia and Solomon [1983]. We neglect the small effect of the positive tropospheric trend on stratospheric mixing ratio gradients and hold the surface boundary region at a uniform 300 ppb (310 ppb is a more appropriate value for current day conditions, but the on-line simulation to which we compared used 300 ppb). Note that due to the linearity of the loss term the mixing ratios of  $\text{N}_2\text{O}$  can be scaled uniformly to any value.

**2.2.3 Ozone.** Ozone chemistry is more complicated than  $\text{CH}_4$  and  $\text{N}_2\text{O}$ .  $P$ ,  $L$ , and  $Q$  are all nonzero and are derived from the CSIRO DTIP two-dimensional chemical transport model (L. K. Randeniya et al., submitted manuscript, 1997). In the lower extratropical stratosphere  $\text{O}_3$  is long enough lived to be a tracer of synoptic and seasonal transport. On the other hand, in the tropical middle and upper stratosphere it is near photochemical equilibrium. There is no tropospheric chemistry in the  $\text{O}_3$  simulations; instead the mixing ratios in surface boundary region are fixed at 20 ppb.

**2.2.4 Sulfur Hexafluoride.**  $\text{SF}_6$  is an anthropogenically produced trace gas of low concentration and extremely long chemical lifetime (the globally integrated estimate of Ravishankara et al. [1993] is 3200 years). Its gradients in the atmosphere are driven by the relatively steady surface source, which has resulted in the approximately linear increase in atmospheric abundance over the past 15 years of about 0.2 parts per trillion per year (ppt/yr) [Maiss et al., 1996; Geller et al., 1997]. The near inertness and linear trend make  $\text{SF}_6$  a powerful tracer of atmospheric motion by allowing deduction of the mean age of stratospheric air [Elkins et al., 1996]; [Harnisch et al., 1996]. In our simulation,  $\text{SF}_6$  is inert ( $P = L = Q = 0$ ), and the uniform surface boundary region increases linearly in time, at the observed mean value.

**2.2.5 Carbon Dioxide.** The atmospheric concentration of  $\text{CO}_2$  has been increasing over the last two centuries, and the average rate of increase in the last 20 years is 1.4 parts per million per year (ppm/yr), although there have been significant interannual variations [Conway et al., 1994]. In addition to the trend there are seasonal variations, having peak-to-peak amplitude as large as 15 ppm, driven by the annual cycle of biospheric uptake and release of carbon. This annual cycle in  $\text{CO}_2$  varies with latitude and is not sinusoidal (see Figure 12 below).

Following the procedure of Hall and Prather [1993], we treat  $\text{CO}_2$  as an inert gas, thereby ignoring the small stratospheric source due to  $\text{CH}_4$  oxidation, and apply

two components as the time-dependent surface boundary condition: (1) a steady 1.4 ppm/yr increase and (2) a latitudinally varying annual cycle. The surface annual cycle is identical to that of Hall and Prather [1993]; it is zonally symmetric and is based on 5 years of observations [Conway et al., 1988]. We run two separate simulations, one with only the trend boundary condition and the other with only the annual cycle boundary condition, and form the  $\text{CO}_2$  distribution by adding the resulting responses. Running two separate simulations enables the propagation of each component to be examined individually (see, for example, Figure 16 below). Note that the distribution of the mean age  $\Gamma$  may be derived from the trend component of  $\text{CO}_2$  just as it is from  $\text{SF}_6$ .

### 3. On-Line Versus Off-Line Transport Modeling

The MACCM2 simulation that generated the winds used to drive the CTM in this study included the two long lived tracers  $\text{CH}_4$  and  $\text{N}_2\text{O}$ , using the same parameterized chemistry scheme (1), boundary conditions, and values of  $L$  as we use in the CTM. To determine the degree of approximation introduced by the off-line technique, we perform simulations of  $\text{CH}_4$  and  $\text{N}_2\text{O}$  with the CTM and compare the results to the on-line distributions. We examine the  $\text{CH}_4$  simulations in this section and discuss the  $\text{N}_2\text{O}$  results in the next section.

Figure 1 compares the zonal mean  $\text{CH}_4$  from the off-line and on-line simulations. There is good agreement between the two simulations: the isopleths have very similar shape and the same seasonal evolution. However, in the lower stratosphere the off-line  $\text{CH}_4$  mixing ratio is higher than the on-line  $\text{CH}_4$ , while in the upper stratosphere the reverse is true. In other words, the vertical gradients of the zonal mean  $\text{CH}_4$  are steeper in the off-line simulation.

The off-line simulation uses the same semi-Lagrangian advection scheme, surface boundary condition, and parameterized chemistry as the on-line simulation, so the differences between the two are due only to differences in the dynamical driving fields. In particular, the off-line simulation (1) uses only daily averaged winds, (2) calculates the vertical velocity by finite differencing of mass continuity (rather than the spectral method of the GCM), and (3) contains no subgrid scale mixing parameterizations. To examine which of these factors are causing the off-line/on-line differences we have performed a series of simulations using data from a second MACCM2 run in which the model output, including the vertical velocity and parameters for convection and vertical diffusion, are archived every 6 hours.

Figure 2 shows the results from five off-line  $\text{CH}_4$  simulations using these data. All simulations were initialized with the September monthly mean  $\text{CH}_4$  from year 5 of the on-line simulation; Figures 2a to 2c show the results of 1-year simulations whereas, Figure 2d shows

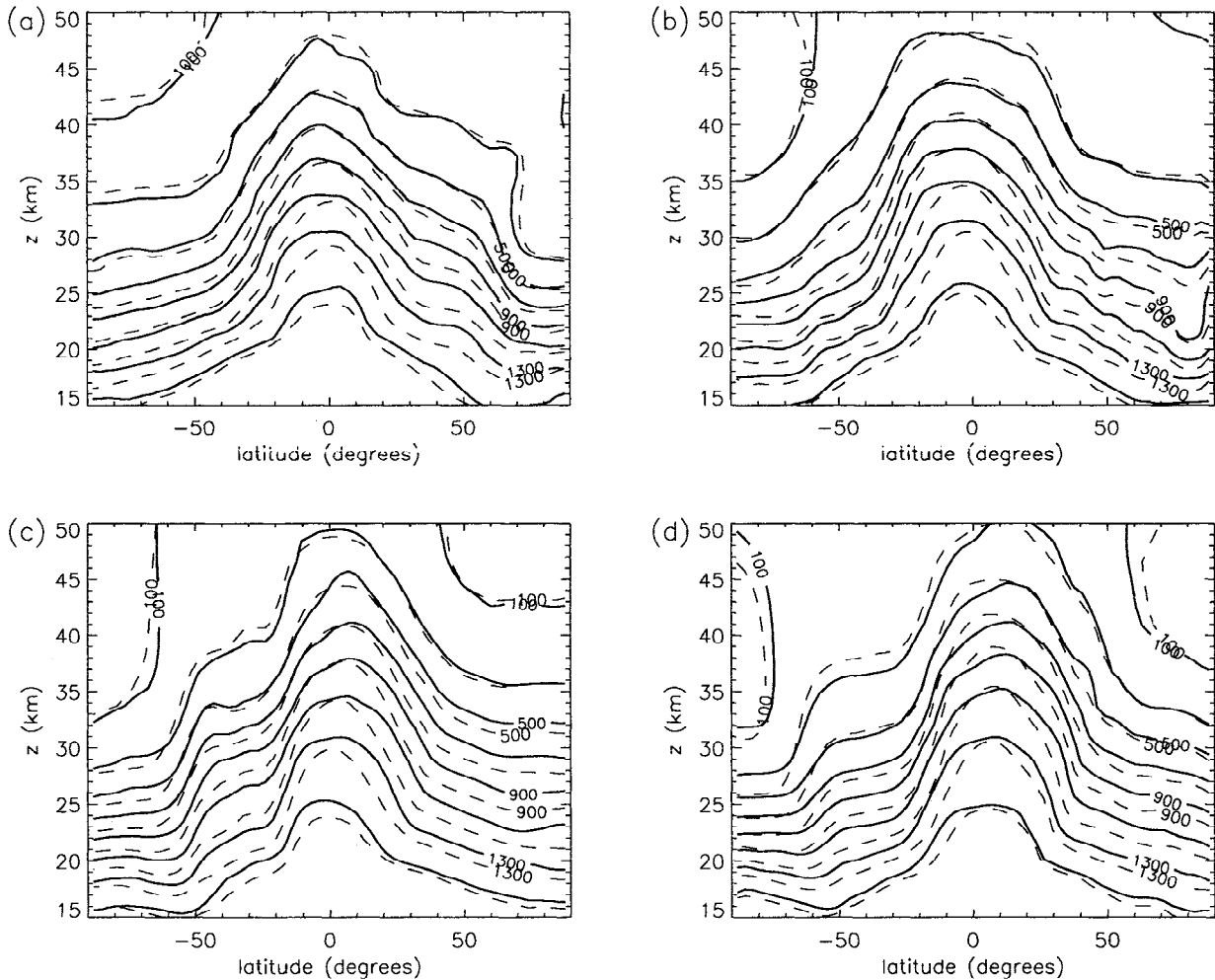


**Figure 1.** Zonal mean  $\text{CH}_4$  from the off-line (solid) and on-line (dashed) simulations at (a) January 19, (b) April 19, (c) July 18, and (d) October 21. The contour interval is 200 ppb.

the results of a 4-month simulation. In all panels the dashed contours represent the off-line simulation using all available data from the GCM (i.e., reading 6-hourly horizontal and vertical wind data and including subgrid scale mixing parameterizations) and the solid contours represent a series of approximations moving away from this simulation. In Figure 2a, the subgrid scale parameterizations, which only occur in the troposphere, have been turned off. Exclusion of these processes makes virtually no difference on the stratospheric  $\text{CH}_4$  distribution; the contours are virtually indistinguishable from the contours with parameterized tropospheric mixing. In Figure 2b the vertical velocity is computed within the CTM using finite differencing of the mass continuity equation, rather than been read from the archived GCM data set. Calculating the vertical velocity within the CTM results in an over estimate of the vertical motion and the isopleths (solid contours) are everywhere above those of the simulation in which the vertical velocity from the GCM is used (dashed contours).

The solid contours of Figure 2c are like those of Figure 2a, but 24-hourly wind averages are used, rather

than 6-hourly averages. Increasing the averaging of the driving fields results in increased vertical gradients, that is, the isopleths in the simulation using 24-hourly averaged data (solid contours) are above (below) those of the 6-hourly simulation (dashed contours) in the lower (upper) stratosphere. This is consistent with the simulations of *Rasch et al.* [1994]: they compared off-line and on-line simulations of the dispersion of the Mount Pinatubo aerosol cloud and showed that there was less dispersion in the off-line simulations using daily averaged winds. This reduced dispersion with increased averaging of the driving fields is presumably because mixing due to transient waves is removed by the averaging. Reduced mixing results in steeper vertical gradients, consistent with the differences between the above  $\text{CH}_4$  simulations.

Comparing Figures 2b and 2c we see that calculating the vertical velocity in the CTM (rather than using that from the GCM) and using daily averaged data (rather than 6-hourly averaged data) have opposite effects on the tracer distributions in the middle and upper stratosphere: calculating the vertical velocity within the

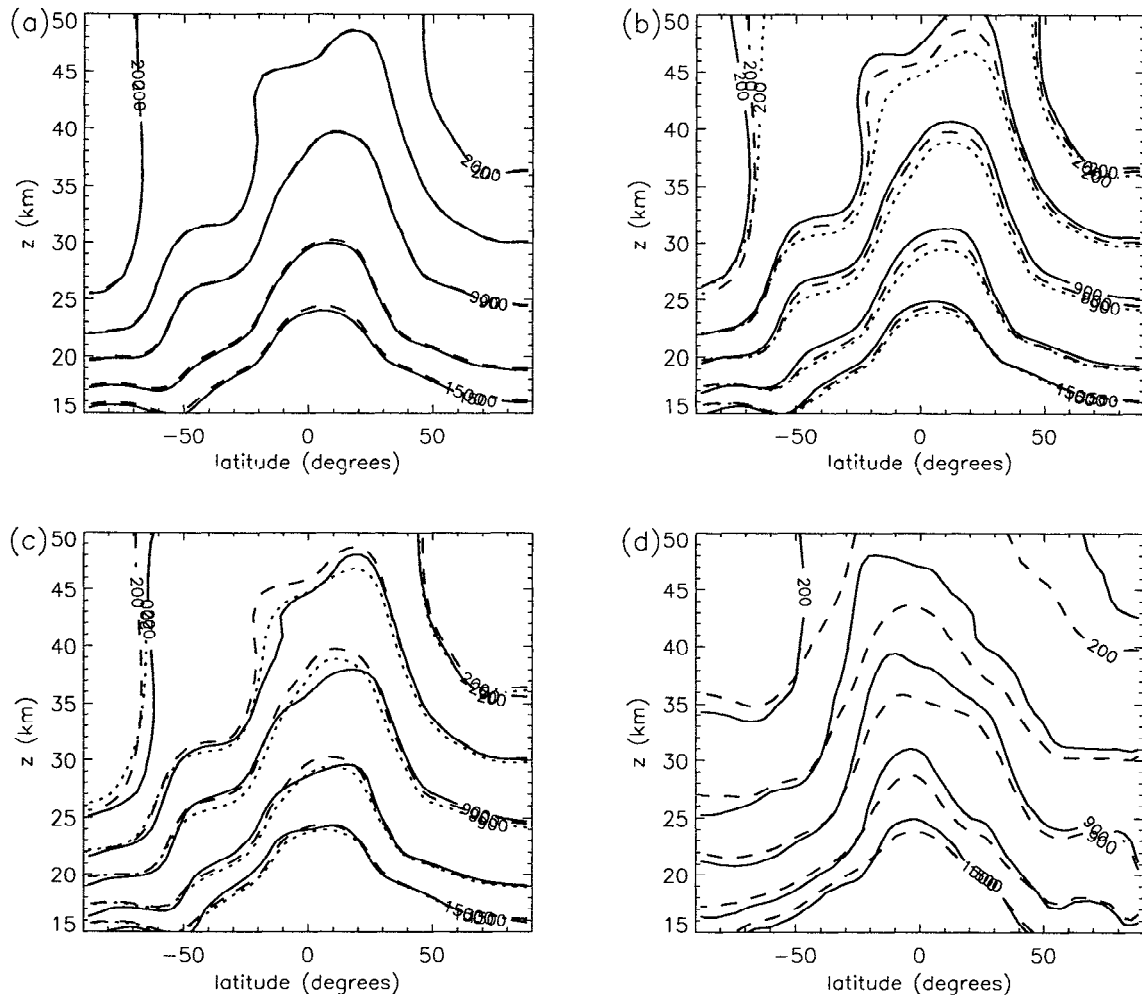


**Figure 2.** Zonal mean  $\text{CH}_4$  from off-line simulations using a second set of MACCM2 winds. The dashed contours are the  $\text{CH}_4$  from an off-line simulation using 6-hourly averaged winds (including the vertical velocity) and subgrid scale parameterisations, while the solid curve is the  $\text{CH}_4$  from off-line simulation using no subgrid scale parameterisations and (a) 6-hourly averaged winds including the vertical velocity, (b) 6-hourly averaged horizontal winds with a vertical velocity computed in the CTM from mass continuity, (c) 24-hourly averaged horizontal winds with the vertical velocity calculated in the CTM, and (d) 6-hourly averaged horizontal winds used every 12 hours. All simulations were initialized with September mean  $\text{CH}_4$  from the on-line MACCM2 simulation; Figures 2a to 2c show September mean distributions after 1 year whereas Figure 2d shows distribution after 4 months (February 1). The dotted contours in Figures 2b and 2c correspond to the on-line  $\text{CH}_4$  distribution.

CTM increases the tracer mixing ratios (moves the isopleths up) whereas using 24-hourly averaged data decreases the tracer mixing ratios (moves the isopleths down). Note however that the difference between calculating or reading in the vertical velocity is much smaller when using daily averaged winds (not shown) instead of 6-hourly averaged winds.

One would expect off-line simulations using all available data from the GCM to be closer to the on-line GCM simulation than off-line simulations using only a subset of the GCM data. However this is not the case for the  $\text{CH}_4$  (and  $\text{N}_2\text{O}$ ) simulations. The September mean on-line  $\text{CH}_4$  from 1 year after the initial date in the off-line simulations is shown by the dotted contours in Figures 2b and 2c. The isopleths in the off-line sim-

ulation using all available data (dashed contour) are above those from the on-line simulation, and there is slightly better agreement with the on-line  $\text{CH}_4$  when 24-hourly data (solid contours in Figure 2c) rather than 6-hourly driving data are used in the off-line simulation. The differences between the off-line simulation using 6-hourly data and the on-line simulation are surprising, and we do not know the cause of these differences. (Note that these differences are not observed in simulations of tropospheric tracers (P. J. Rasch et al., submitted manuscript, 1997).)

Another issue relevant to off-line simulations is whether to use averaged or instantaneous wind data. Both introduce inaccuracies compared to the on-line simulation: averaging removes transients, while instantaneous

subsampling of the wind data in general results in aliasing of fluctuations at frequencies higher than the sampling rate. Although we do not have instantaneous data from MACCM2, we can investigate the effect of subsampling by using the 6-hourly averaged data every 12 or 24 hours. Figure 2d shows the results of a 4-month simulation using 6-hourly averaged winds every 12 hours (solid contours). There is a large difference between this simulation and those using 6-hourly averaged winds every 6 hours (dashed contours), particularly in the upper stratosphere, where there is spurious upward motion, resulting in the larger values of CH<sub>4</sub> in the upper stratosphere. This spurious motion is even larger if the 6-hourly averaged winds are used only every 24 hours (not shown). We have also performed an off-line simulation of N<sub>2</sub>O using instantaneous winds from the Geophysical Fluid Dynamics Laboratory "SKYHI" GCM every 12 hours (not shown), and comparisons with the on-line N<sub>2</sub>O from the SKYHI GCM also show spurious upward movement of the N<sub>2</sub>O isopleths. These comparisons suggest that the use of instantaneous data, such as data from meteorological assimilation systems, in off-line CTMs requires a sampling frequency greater than once per 12 hours, and perhaps greater than once per 6 hours.

In all of the off-line simulations in which the vertical velocity is calculated within the CTM a spatial filter has been applied to the vertical velocity calculated from mass continuity. Without this filter spurious vertical motion occurs at the poles (because of errors in the calculation of the vertical velocity near the pole). We apply a running mean filter around a latitude circle in which the number of grid points used in the filter varies with latitude. By performing simulations using filters with different latitudinal extent we found there was almost no difference between (1) using a filter which only applies to the polar-most latitude and replaces the vertical velocity at each longitude with the zonal mean value and (2) using a filter starting at 65° and in which the number of averaged longitudes increases from 3 at 65° to 128 (complete zonal averaging) at the polar-most latitude.

## 4. Comparison to Observations

In this section we examine the zonal mean structures of the simulated CH<sub>4</sub>, N<sub>2</sub>O, O<sub>3</sub>, SF<sub>6</sub>, and CO<sub>2</sub>, and compare them to observations and previous simulations.

### 4.1 Methane

The solid contours in Figure 3 show the monthly mean zonal mean CH<sub>4</sub> from a climatology using data from the Cryogenic Limb Array Etalon Spectrometer (CLAES) and the Halogen Occultation Experiment (HALOE) instruments aboard the Upper Atmosphere Research Satellite (UARS) [Randel *et al.*, 1997]. In this climatology the CH<sub>4</sub> averaging is performed with potential vorticity (PV), rather than geographic latitude,

as the horizontal coordinate. The PV is then mapped to "equivalent latitude," the latitude at which the area encompassed in the polar cap is equivalent to that encompassed by the PV circle. The equivalent PV latitude is only significantly different from the geographic latitude in northern high latitudes where the Arctic polar vortex is often disturbed and off the pole, and so the PV contours deviate greatly from zonal circles. In this combined climatology CLAES data are used to fill the regions not sampled by HALOE (winter polar regions); see Randel *et al.* [1997] for details.

Comparing this CH<sub>4</sub> climatology with the off-line simulation (dotted contours) we see that there is general agreement in the structure and seasonal variability of the modeled and observed isopleths. In particular, there are steep gradients at the edge of the tropics, whose location shifts with season, and at the edges of the winter polar vortices. However, there are some significant discrepancies: (1) in the simulated CH<sub>4</sub> there is no double-peak structure in the tropical upper stratosphere, (2) the model over-estimates the mixing ratio within the Antarctic polar vortex (see Figure 4), and (3) the model generally underestimates the CH<sub>4</sub> abundance throughout the upper stratosphere (see Figure 4). Discrepancy 1 is a consequence of the weak SAO in the dynamics of the MACCM2 [Sassi *et al.*, 1993; Boville, 1995], while discrepancy 2 is due in part to weak descent within the Antarctic polar vortex [Garcia and Boville, 1994; Boville, 1995]. In addition, overestimation of mixing ratios inside the vortex could, in part, be caused by insufficient isolation of the vortex from mid-latitudes. The explanation for discrepancy 3 is not yet clear. We have performed CH<sub>4</sub> simulations both with different loss coefficients (from the CSIRO DTIP two-dimensional chemical transport model (L. K. Randeniya *et al.*, submitted manuscript, 1997)) and with a different CTM [Prather *et al.*, 1987], driven by winds from the GCM of the Goddard Institute for Space Studies, and found qualitatively similar underestimates of upper stratospheric mixing ratios.

Our off-line simulation of CH<sub>4</sub> using chemistry as parameterized by mean production and loss fields is very similar to the CH<sub>4</sub> from the on-line MACCM2 simulation using explicit chemistry (multiple interacting species) of Rasch *et al.* [1995]. The similarities and discrepancies of the model with observations described above are similar to those presented by Rasch *et al.* [1995].

### 4.2 Nitrous Oxide

Figure 5 shows the zonal mean N<sub>2</sub>O from both on-line (dashed contours) and off-line (solid) simulations. The general shape of the isopleths and the difference between the off-line and on-line simulations is similar to that of the CH<sub>4</sub> simulations. The on-line N<sub>2</sub>O is the same as examined by Randel *et al.* [1994] and is very similar to the N<sub>2</sub>O simulation of Rasch *et al.* [1995]. Both these studies compared the model N<sub>2</sub>O with ob-

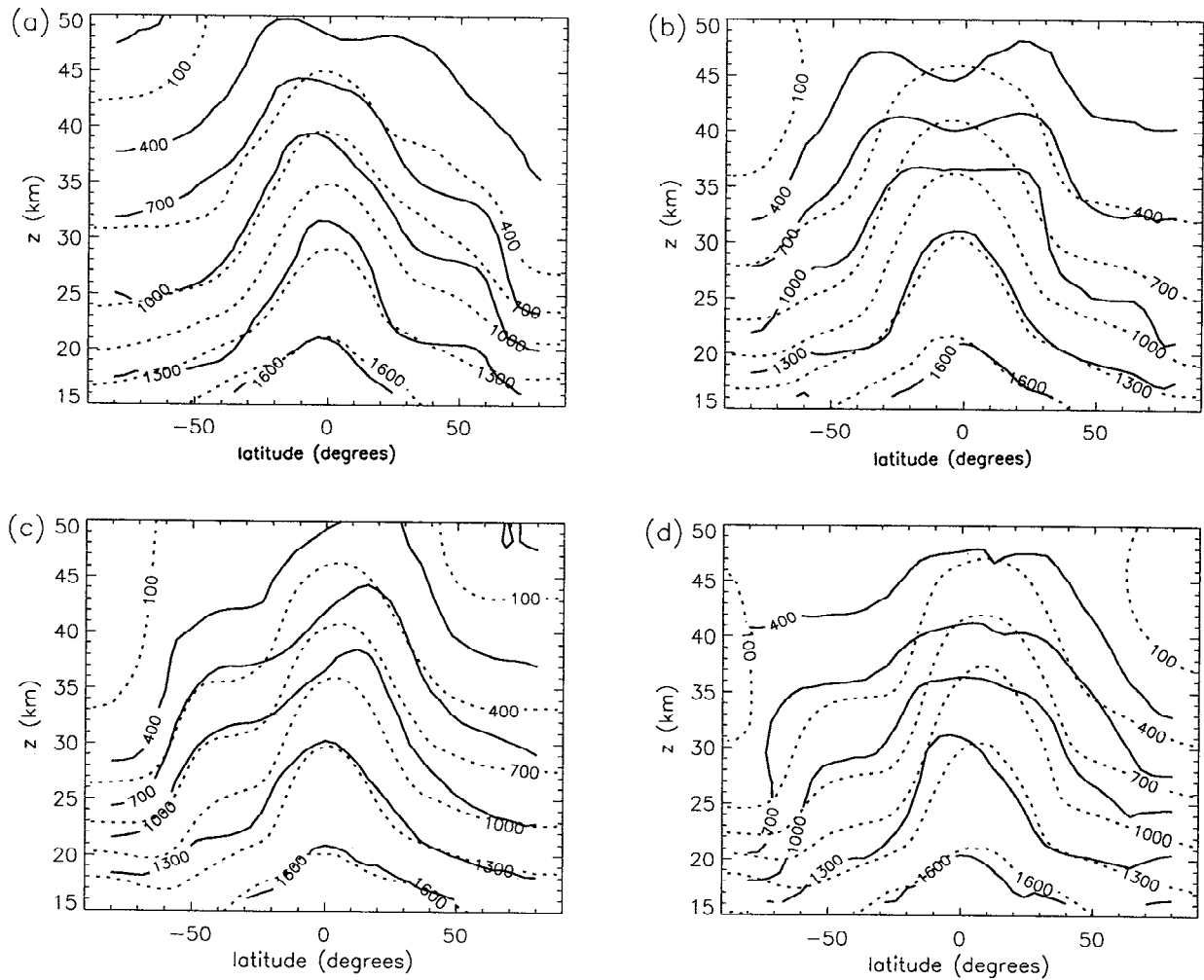


**Figure 3.** Monthly mean zonally averaged CH<sub>4</sub> from a HALOE/CLAES climatology (solid contours) and from the CTM (dotted) for (a) January, (b) April, (c) July, and (d) October. Contour intervals are 300 ppb. See text for further discussion.

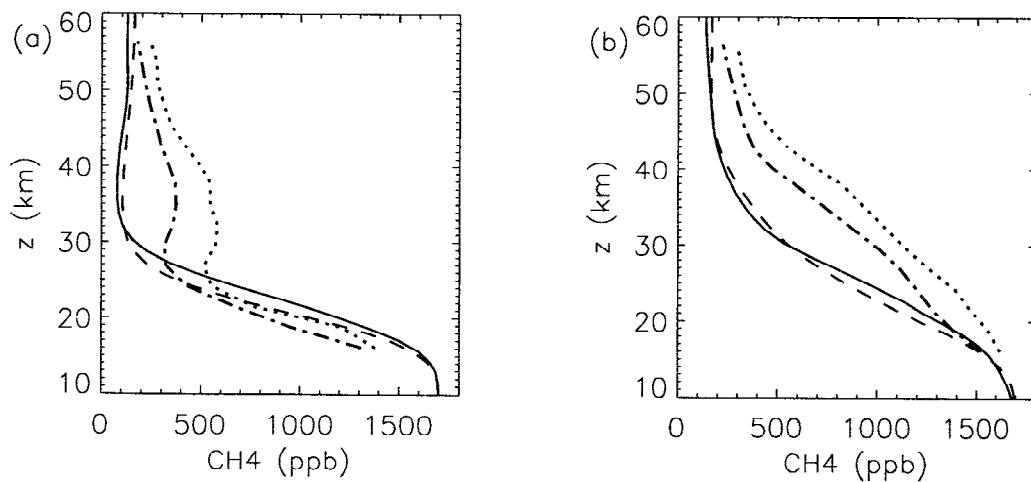


**Figure 4.** October mean zonal mean vertical CH<sub>4</sub> profiles from the off-line (solid) and on-line (dashed) simulations and from HALOE (dash-dot) and CLAES (dotted) October climatology. The latitudes are (a) 76°S and (b) 44°S.

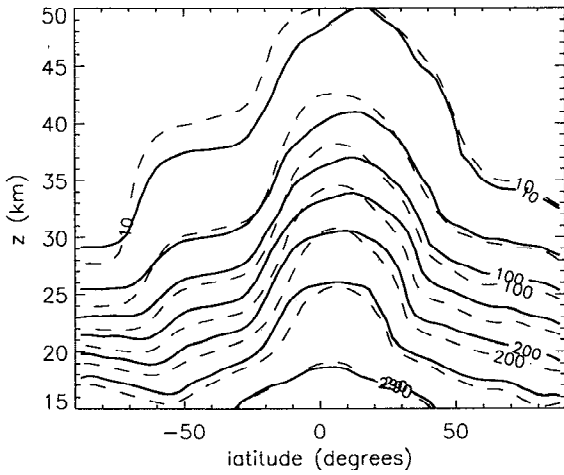


**Figure 5.** Zonal mean  $N_2O$  from the off-line (solid) and on-line (dashed) simulations at October 21. Contour levels are 10, 50, 100, 150, 200, and 250 ppb.

servations (*Randel et al.* [1994] with CLAES and *Rasch et al.* [1995] with Atmospheric Trace Molecule Spectroscopy (ATMOS) and Stratospheric and Mesospheric

Sounder (SAMS)) and showed the same general agreement and deficiencies as discussed above with the  $CH_4$  simulation.

**4.3 Ozone**

Figure 6 shows the monthly mean zonal mean  $O_3$  from the model and from a climatology based on 5 years of observations from the Microwave Limb Sounder (MLS) on UARS, for January and July. This climatology is constructed using the same statistical analysis given by *Randel et al.* [1997]. The simulation has many realistic features: the maximum volume mixing ratio of around 10 ppm occurs in the tropical mid-stratosphere, and the strong vertical gradients in the lower stratosphere, particularly the tropics, are well represented. However, there are significant differences in the vertical profiles. These differences are clearly shown in Figure 7, which compares model profiles with monthly mean profiles from MLS, HALOE and Stratospheric Aerosol and Gas Experiment (SAGE) II climatologies. At all latitudes there is a misalignment of the vertical maximum; in the tropics the model peak is 2 to 5 km too low, and

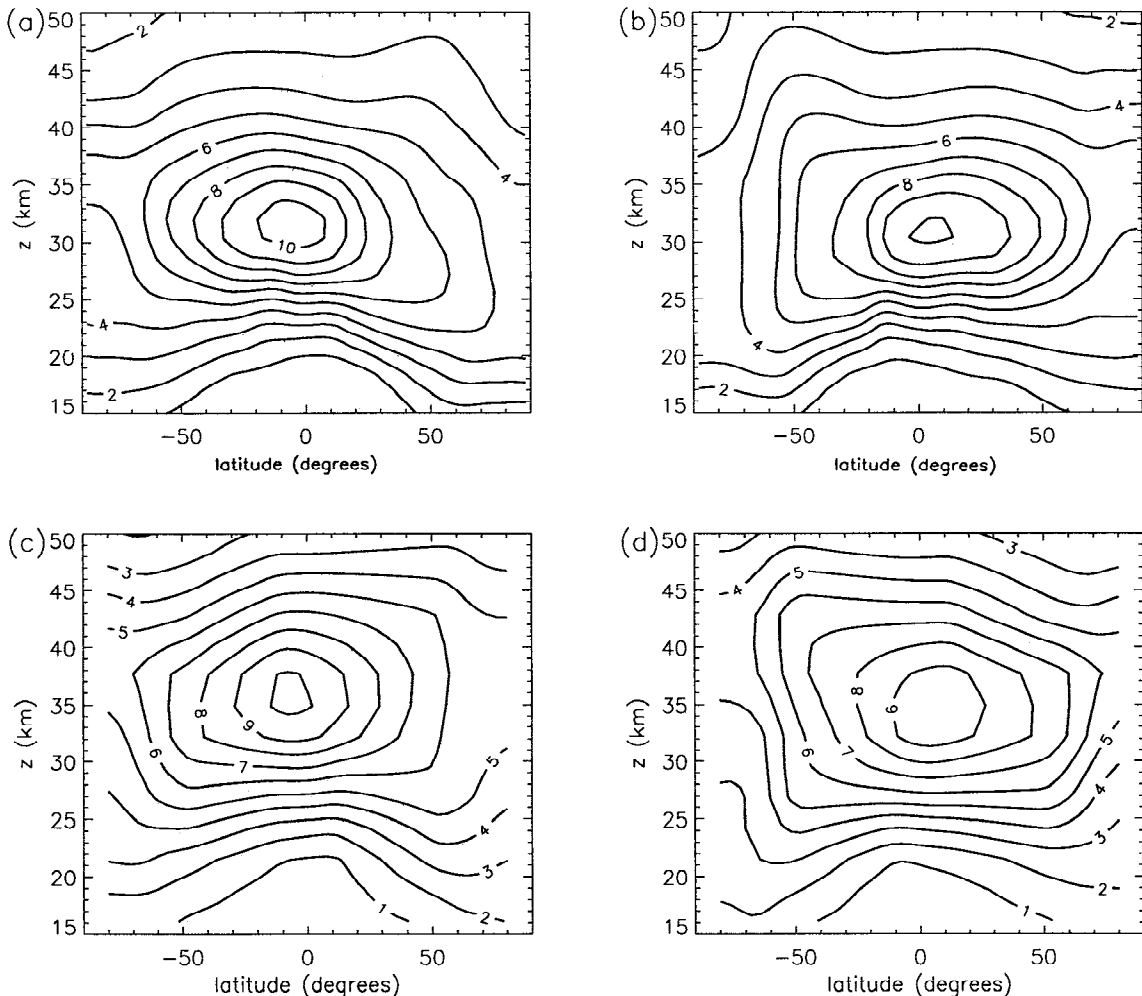


**Figure 6.** Zonal mean  $O_3$  distributions for (a) January and (b) July from the CTM, and for (c) January and (d) July from an MLS climatology. The contour interval is 1 ppm.

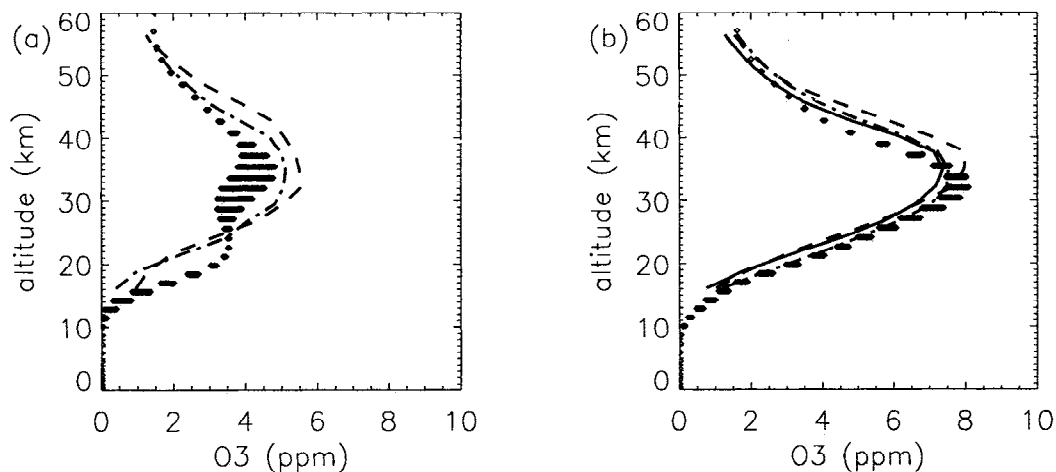


**Figure 7.** Monthly mean vertical  $O_3$  profiles from the CTM (symbols), HALOE (solid), MLS (dashed), and SAGE II (dot-dash) for October at (a)  $76^\circ\text{S}$  and (b)  $44^\circ\text{S}$ . The CTM values are plotted at all 128 model longitudes. The observational profiles represent zonal composites from the climatologies.

the vertical structure is significantly different at high latitudes. This misalignment of the vertical maximum is a common problem in both two-dimensional [Remsberg and Prather, 1993] and three-dimensional [Rasch *et al.*, 1995; Eckman *et al.*, 1995] models.

The latitudinal and temporal variation of the model and observed column-integrated  $O_3$  is shown in Figure 8. The model's column  $O_3$  has many realistic features: there is good agreement in the magnitude, location, and timing of the peak values at high latitudes in both the northern and southern hemisphere, and in the seasonal evolution of the tropical minimum. There are, however, some discrepancies: the tropical values are slightly lower than observed, and the breakup of low values in October southern polar regions occurs in November in the model. The problems in the southern polar region are due to known deficiencies in the MACCM2 simulation of the Antarctic polar vortex: the polar jet is too strong and the winter-to-summer transition is delayed by about 1 month [Boville, 1995].

It is interesting to compare our simulation with the on-line  $O_3$  simulation of Rasch *et al.* [1995], in which an explicit photochemistry scheme was used, rather than the mean production and loss fields of these simulations. Even though the two simulations treated the  $O_3$  chemistry differently, the resulting  $O_3$  fields are very similar, and both simulations have the deficiencies mentioned above. It is curious that certain aspects of our simulation are, in fact, more realistic than the simulation of Rasch *et al.* [1995]. The model's ozone deficit compared to observations at 40 km is smaller, and the magnitudes of the peak total column values in both northern and southern hemispheres agree better with TOMS.

#### 4.4 Sulfur Hexafluoride

As  $SF_6$  is inert and linearly increasing with time in our simulation, the time the concentration at a given

location  $\mathbf{x}$  lags that of a reference location  $\mathbf{x}_0$  is the mean age  $\Gamma(\mathbf{x}, \mathbf{x}_0)$ ; typically  $\mathbf{x}_0$  is chosen at the surface or at the tropical tropopause. Figure 9 shows the zonal mean  $\Gamma$ , relative to the surface, from the  $SF_6$  simulation: the youngest stratospheric air is just above the tropical tropopause (approximately 0.5–0.8 years older than the surface), while the oldest is at the winter pole of the upper stratosphere (older than 10 years at 40 km at the southern winter pole). The shape of the  $\Gamma$  surfaces are qualitatively similar to those of  $CH_4$  and  $N_2O$ : they bulge up in the tropics and down at the winter pole. However, whereas the gradients in  $CH_4$  and  $N_2O$  are driven by photochemical destruction in the middle and upper stratosphere, the gradients in  $SF_6$  (and also  $CO_2$ , see below) are driven by the time-varying tropospheric mixing ratio. A careful comparison of  $\Gamma$  and  $N_2O$  (or  $CH_4$ ) distributions reveals that there are in fact differences in the shapes of the zonal mean contours at the edge of the polar vortices and at the edges of the tropics. (See Hall and Prather [1995] for further discussion; their " $CO_2^T$ " tracer is equivalent to our  $SF_6$ .)

There are no satellite observations of  $SF_6$ , or any other linearly increasing tracer, so we do not have direct global measurements of age throughout the stratosphere. However, in recent years  $SF_6$  measurements have been made aboard aircraft [Elkins *et al.*, 1996], balloons [Harnisch *et al.*, 1996; Patra *et al.*, 1997], and the space shuttle [Rinsland *et al.*, 1993], thus providing measurements of the mean age in certain regions of the stratosphere. The mean age of air can also be derived from  $CO_2$  measurements [e.g., Bischof *et al.*, 1985; Boering *et al.*, 1996], although the effect of the annual cycle in tropospheric abundance needs to be accounted for in the lower stratosphere [Hall and Prather, 1993; Boering *et al.*, 1996].

In situ measurements of  $SF_6$  and  $CO_2$  have been made from  $70^\circ\text{S}$  to  $60^\circ\text{N}$  in the lower stratosphere aboard the

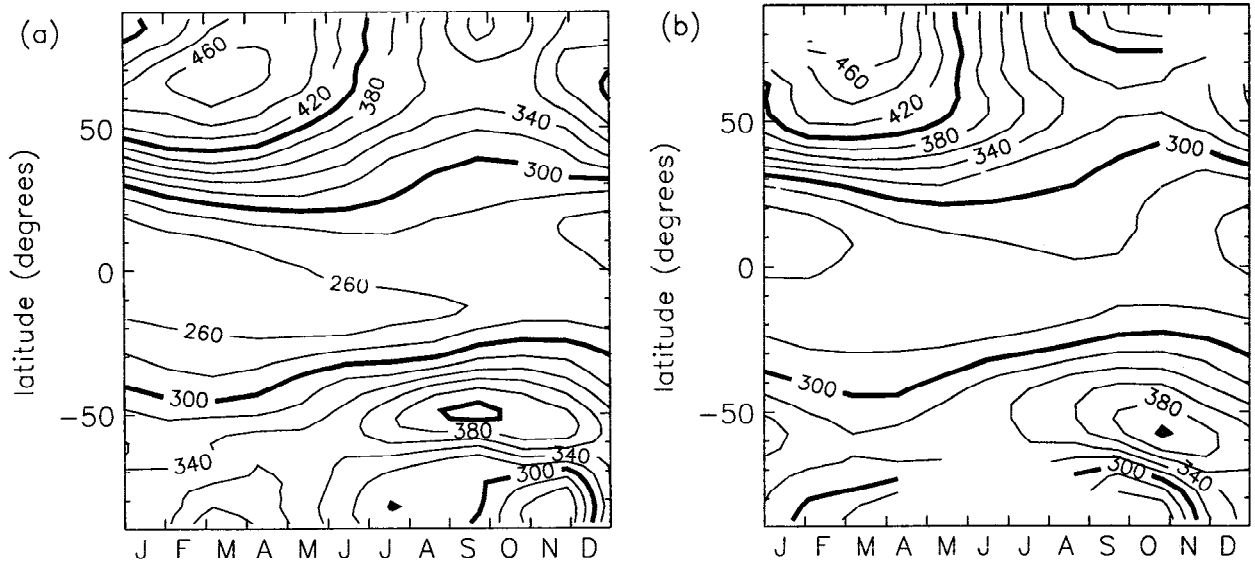


**Figure 8.** Latitude-time contours of zonal mean monthly mean column O<sub>3</sub> (Dobson units) from (a) the CTM and (b) from a 5 year climatology (1979-1984) from the TOMS instrument (version 6).

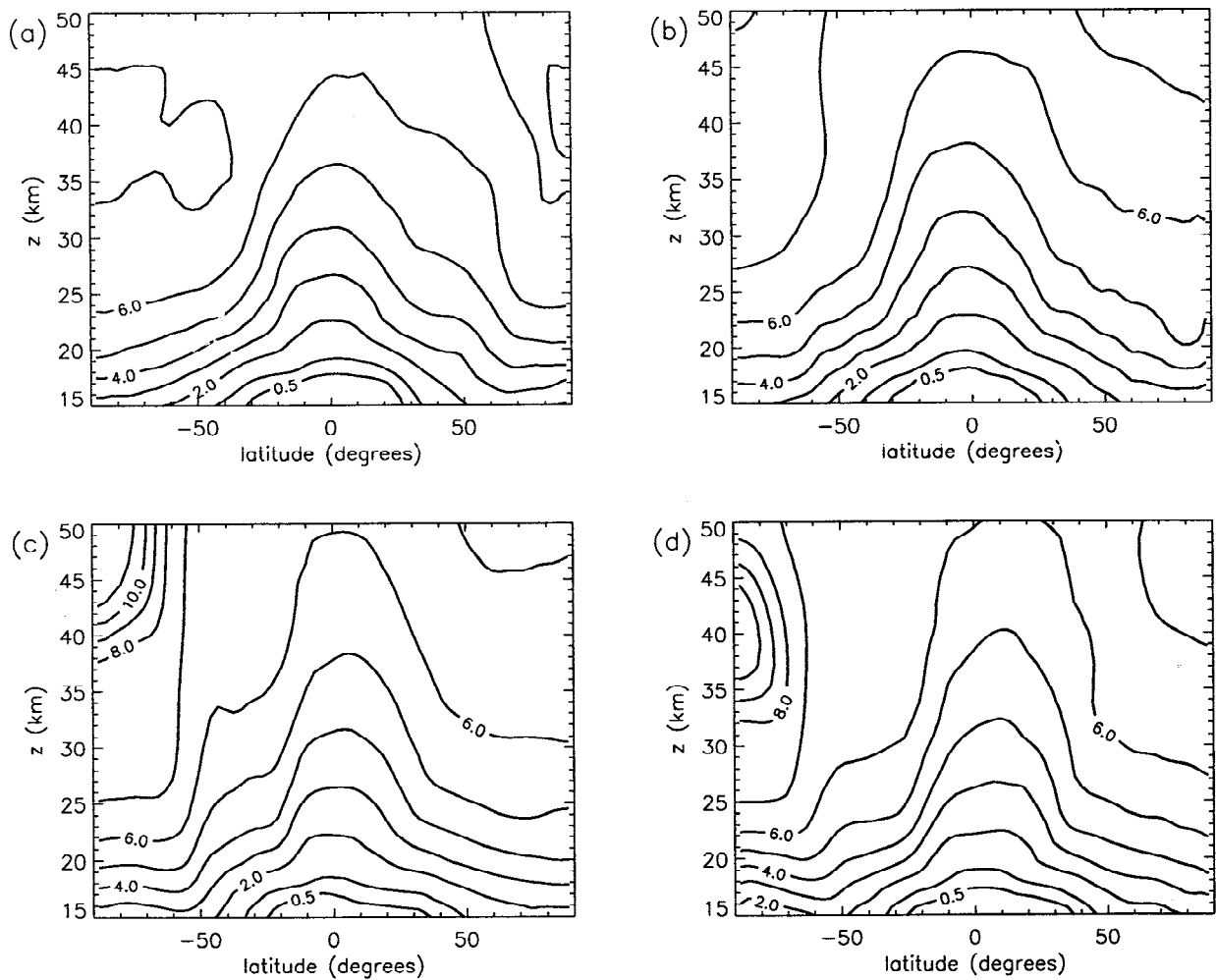


**Figure 9.** Monthly mean zonal mean  $\Gamma$  (mean age) calculated from the CTM simulations of SF<sub>6</sub> for (a) January, (b) April, (c) July, and (d) October. Contour levels are 0.5, 1.0, 2.0, 3.0 ... 10.0 years.

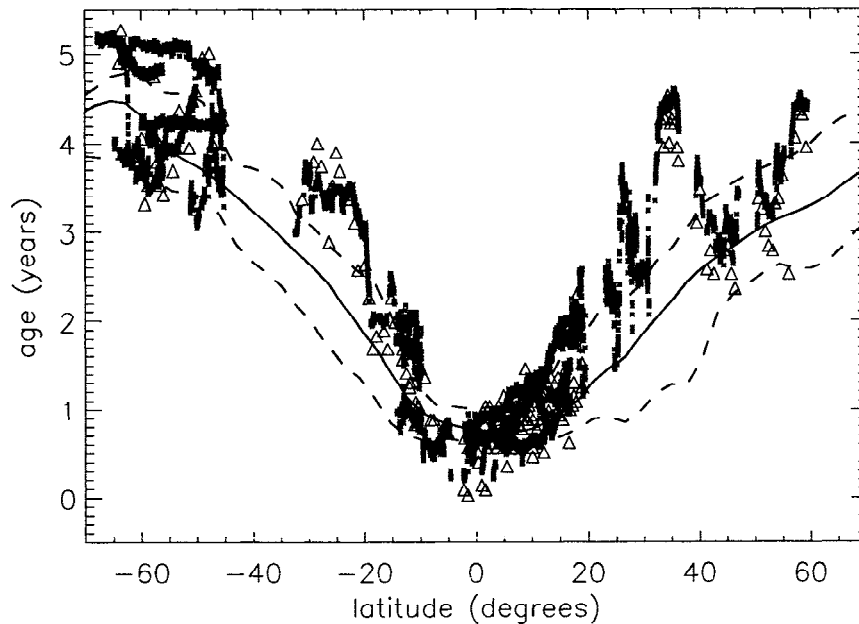


**Figure 10.** Variations of  $\Gamma$  with latitude in October from the CTM (curves) and aircraft measurements (symbols). The solid curve is the zonal mean model value at  $z = 19.8$  km on October 21, while dashed curves are the minimum and maximum values around a latitude circle at this altitude. The symbols are mean age derived from measurements of  $\text{SF}_6$  (triangles) and  $\text{CO}_2$  (solid squares) from October and November 1994. The uncertainty in  $\Gamma$  from both measurements is around 0.2 and 0.3 years [Boering et al., 1996; (C. M. Volk et al., submitted manuscript, 1997)]. In this plot, age is calculated relative to the tropical tropopause.

NASA ER2 aircraft [Elkins et al., 1996; Boering et al., 1996]. Figure 10 compares the model  $\Gamma$  at 19–21 km with that deduced from the aircraft measurements of  $\text{SF}_6$  (triangles) and  $\text{CO}_2$  (solid squares) in late October and early November 1994. Note that in this plot the age, from both the model and observations, is relative to the tropical tropopause.  $\Gamma$  is calculated from the  $\text{SF}_6$  and  $\text{CO}_2$  measurements by determining the time lag of the stratospheric measurements from linear fits to the time series of the tracers at the tropical tropopause. The global mean surface time series from Geller et al. [1997] is used for  $\text{SF}_6$ , and the time lag from this surface value is converted to a lag from the tropical tropopause by subtracting 0.8 years; this is the time lag between the average tropical upper tropospheric  $\text{SF}_6$  mixing ratio measured aboard the ER2 during the above period and the global mean surface time series. The mean age is determined from  $\text{CO}_2$  as given by Boering et al. [1996]: a linear fit to the deseasonalized boundary condition for  $\text{CO}_2$  in air entering the stratosphere derived from ER2 observations from 1992 to 1996 is used as the reference, and a correction for  $\text{CH}_4$  oxidation is included. The uncertainties for the age derived from both measurements are around 0.2 to 0.3 years [Boering et al., 1996, (C. M. Volk et al., On the evaluation of source gas lifetimes from stratospheric observations, submitted to *Journal of Geophysical Research*, 1997; hereinafter referred to as submitted manuscript)], and the two values agree within this limit (even within the tropics where

the annual cycle in  $\text{CO}_2$  may have been expected to affect the age from  $\text{CO}_2$ ). It should be noted that neither the time series of global mean surface  $\text{SF}_6$  or annual mean  $\text{CO}_2$  are exactly linear with time, and this non-linearity affects the age-of-air calculation. Volk et al. (submitted manuscript, 1997) has estimated this effect for the mean age derived from the  $\text{SF}_6$  measurements and get slightly older values than the above simple time lag (around 0.5 years for the oldest air sampled). Note that this uncertainty is larger than that due to measurements uncertainties.

The modeled  $\Gamma$  agrees well with the measurements, although the latitudinal gradient in the model is slightly smaller than observed. Within the tropics,  $\Gamma$  in both the model and observations is around 1 year, whereas in middle to high latitudes the modeled  $\Gamma$  ranges from 2.5 to 4.5 years compared to the observations of 3 to 5 years.

In addition to the above lower stratospheric measurements, altitude profiles of mean age have been derived from balloon-based measurements of  $\text{SF}_6$  and  $\text{CO}_2$ . Figure 11 compares the model  $\Gamma$ , relative to the surface, with that derived from the  $\text{SF}_6$  measurements of Harnisch et al. [1996]. The agreement between the model and measurements at low and middle latitudes is very good, with  $\Gamma$  at 30 km varying between 4.5 and 6 years from low to middle latitudes. There is, however, a difference between the model and measurements for the wintertime values at high latitudes. The measurements

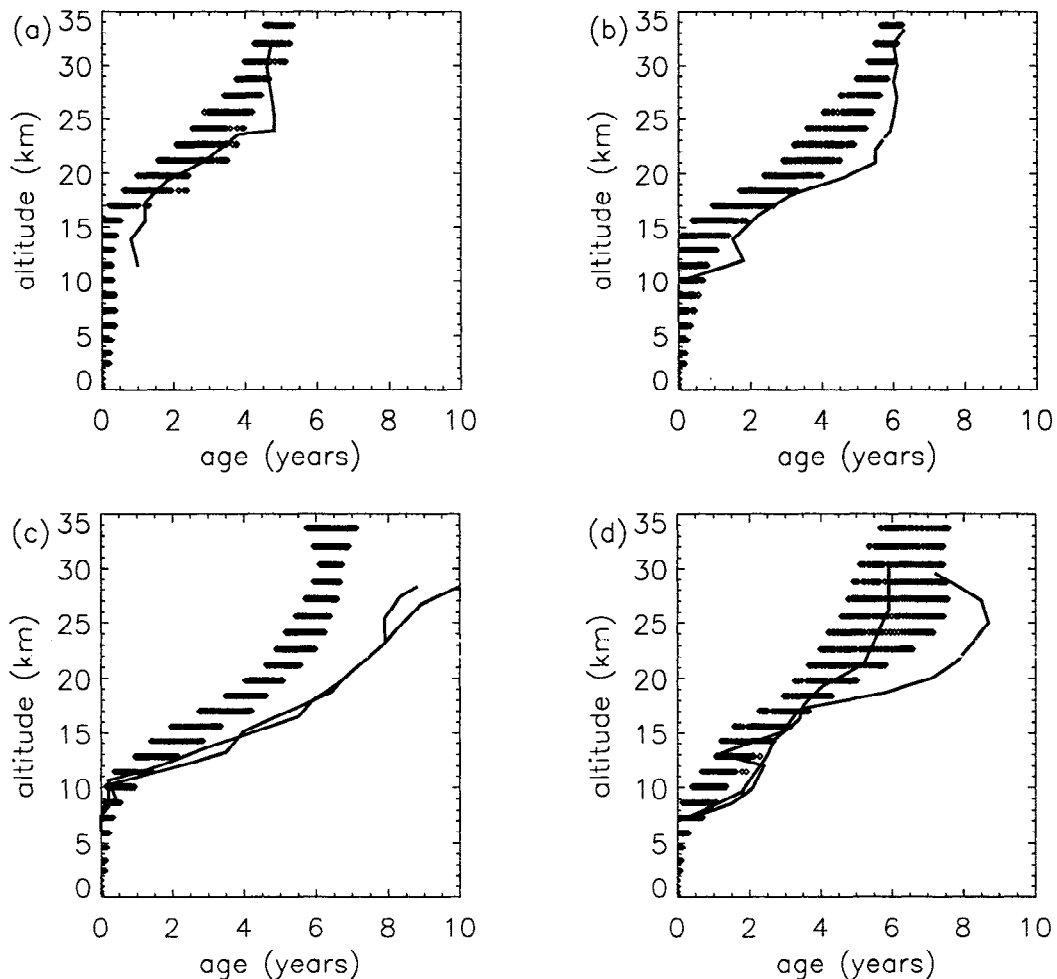


**Figure 11.** Profiles of mean age versus altitude calculated from the CTM-simulated SF<sub>6</sub> (symbols) and balloon measurements of SF<sub>6</sub> (curves). Observations were made at (a) 17°N (March 25), (b) 44°N (September 30), (c) 68°N (January 18, February 6), and (d) 68°N (March 7, March 20). The model values correspond to the nearest archived dates and latitudes to these observations, and values are plotted at all 128 longitudes.

yield  $\Gamma$  as old as 10 years at 30 km whereas the oldest air in the model at this altitude is only around 8 years old. Note that the measurements in January and February at 68°N are inside the polar vortex. Another difference between the model and measurements is the vertical gradients at low and middle latitudes: the measurements show, in the tropics and middle latitudes, a distinct transition from a region of steep vertical gradients in the lower stratosphere to a region of weak or no vertical gradient commencing around 25–30 km (e.g., Figures 11a and 11b); the vertical gradients of the model's age vary more gradually.

Note that when calculating  $\Gamma$  from the above aircraft and balloon SF<sub>6</sub> measurements the influence of mesospheric loss has not been taken into account. Preliminary calculations indicate that this loss affects the time lag between the middle stratosphere and troposphere, and that the above estimates of  $\Gamma$  are likely to be larger than the true  $\Gamma$ .

The mean ages derived other balloon measurements of SF<sub>6</sub> [Patra et al., 1997] and CO<sub>2</sub> [Bischof et al.,

1985; Schmidt and Khedim, 1991; Nakazawa et al., 1995] are consistent with the above measurements: these measurements yield mean ages of around 5 to 6 years for air at 30 km in northern midlatitudes and also show very weak vertical gradients above 25–30 km.

The simulated  $\Gamma$  in Figure 9 also agrees well with other estimates: ATMOS/ATLAS 1 measurements of SF<sub>6</sub> during March at 24 km in southern midlatitudes [Rinsland et al., 1993] yield  $\Gamma \approx 5.5$  years, ER2 flask sample measurements of CFC-115 in northern high latitudes of the lower stratosphere during January 1989 [Pollock et al., 1992] yield  $\Gamma \approx 4.4$  years, and ER2 flask sample measurements of CO<sub>2</sub> and CFC-115 in the lower stratosphere during the 1991/1992 winter [Daniel et al., 1996] yield  $\Gamma = 3$ –4 years outside the Arctic vortex and 5–6 years inside the vortex.

It is important to note that the  $\Gamma$  in our simulation is much older, particularly in the upper stratosphere and at high latitudes, than both the three-dimensional simulation of Hall and Prather [1993] and several two-dimensional models [Bacmeister et al., 1995; K. Ryan,

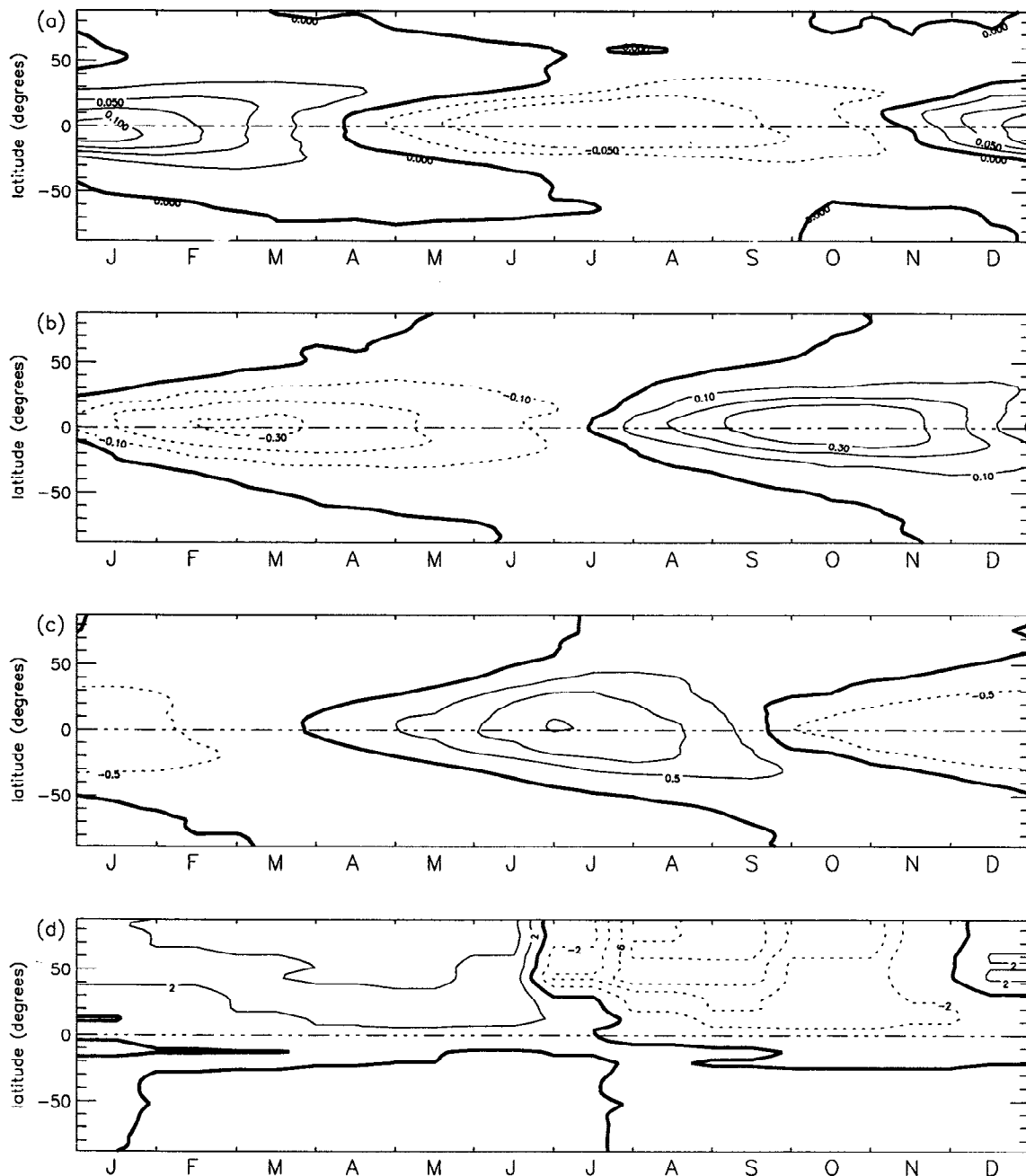


**Figure 12.** The zonal average of the simulated annual  $\text{CO}_2$  cycle at (a) 24 km, (b) 19.8 km, (c) 15.6 km, and (d) the surface (the time-dependent boundary condition). The contour levels are labeled in ppm, and represent deviations from the annual mean. The bold curve is the zero contour.

personal communication 1996; M. Ko, personal communication 1996]. The above measurements (in particular the measurements of *Harnisch et al.* [1996] revealing ages as great as 10 years) suggest our simulation is more realistic than these other simulations.

#### 4.5 Carbon Dioxide

The response to the steady linear increase of our  $\text{CO}_2$  simulation is identical to the  $\text{SF}_6$  simulation discussed in the previous section. The mean age  $\Gamma$  is deduced from

any linearly increasing conserved tracer. However, the annual cycle component of the  $\text{CO}_2$  simulation is an additional diagnostic of model transport.

The variation of the simulated annual cycle with latitude and time at the surface (the boundary condition in the model) and several altitudes is shown in Figure 12. The phase shifts both with altitude (a shift of the maximum of about 6 months from 15.6 to 24.1 km) and with latitude (a shift of the zero anomaly contour of about 3 months from equator to pole at 15.6 km). As discussed

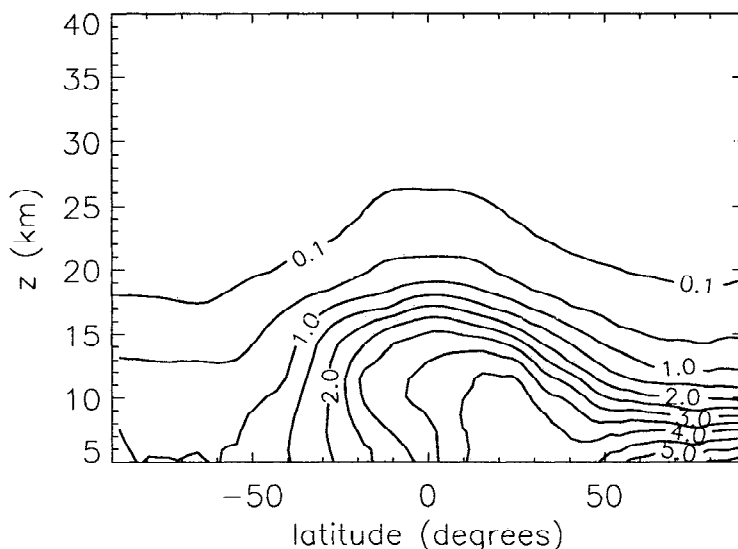


**Figure 13.** The zonal mean peak-to-peak amplitude of the simulated CO<sub>2</sub> annual cycle versus latitude and altitude. The contour levels are 0.1, 0.5, 1.0, 1.5 ... ppm.

by *Hall and Waugh* [1997] this propagation time is a different, shorter timescale than the mean age. As the cycle propagates vertically (by advection in the tropics and quasi-horizontal transport into midlatitudes), the amplitude is rapidly attenuated. The zonally averaged peak-to-peak amplitude versus latitude and altitude is shown in Figure 13. At the surface in northern midlatitudes the amplitude is as large as 14 ppm, but by the tropical tropopause ( $\approx 17$  km) the amplitude is attenuated to about 2 ppm. The amplitude attenuates even more rapidly with altitude within the stratosphere, and in midlatitudes at 20 km it is less than 0.1 ppm.

Our simulated CO<sub>2</sub> cycle is qualitatively similar to that of *Hall and Prather* [1993], as can be seen by comparing our Figure 12 to their Figure 5. However, the cycle of *Hall and Prather* [1993] attenuates less rapidly with height in the stratosphere. Comparing our Figure 13 with their Figure 4, the 0.5 ppm cycle amplitude contour in the *Hall and Prather* [1993] simulation and the 0.1 ppm contour in our simulation are at ap-

proximately the same altitude. The difference in the attenuation of annual cycles between these two models is discussed further by *Hall and Waugh* [1997].

The realism of our stratospheric simulation depends in part on the representation of the CO<sub>2</sub> annual cycle at the tropical tropopause, which forces the stratosphere. Thus, it is important to check the model's tropopause cycle against observations. Over the last 4 years, in-situ measurements of CO<sub>2</sub> have been made in the upper troposphere and lower stratosphere at several different times of year, and from these measurements it is possible to estimate the phase and amplitude of the CO<sub>2</sub> cycle at the tropical tropopause [*Boering et al.*, 1996]. Figure 14 shows the simulated annual cycle near the equator at 15.6 km ( $\approx 340$  K) and 17 km ( $\approx 390$  K), together with ER2 measurements of CO<sub>2</sub> at 380-390 K [*Boering et al.*, 1996; Figure 3]; the deseasonalized boundary condition determined by the measurements has been subtracted from the CO<sub>2</sub> measurements to yield the annual cycle independent of the increasing

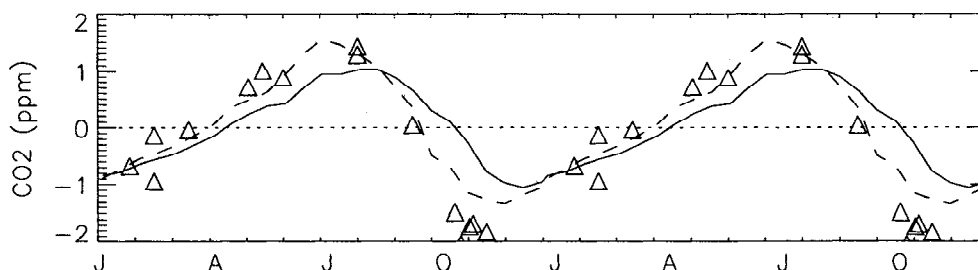


**Figure 14.** The annual CO<sub>2</sub> cycle near the tropical tropopause from simulations and from aircraft measurements. The curves are the simulated cycle at 15.6 km (dashed) and 17.0 km (solid). Symbols correspond to ER2 measurements with annual trend removed at a potential temperature of 390 K made between November 1992 and February 1996. The long term precision (flight-to-flight and mission-to-mission) of the measurements is  $\pm 0.05$  ppm [*Boering et al.*, 1996]. A single annual cycle has been repeated twice for clarity. See text for details.

trend. At 17 km the simulated peak-to-peak amplitude of CO<sub>2</sub> is 2 ppm versus the observed 3 ppm (the modeled 15.6 km value is close to 3 ppm), and the phase lags that observed by about 1 month. These differences suggest that the model transport from the surface to the tropical tropopause is too slow, which might be expected in a simulation such as ours, with no subgrid scale parameterized mixing. Indeed, simulations with data from the second MACCM2 run discussed in section 3 show better agreement when subgrid scale mixing is included in the simulation. Note that discrepancies in our simulations could also arise from errors in the CO<sub>2</sub> climatology used as the model's surface boundary condition.

Figure 15 compares vertical profiles of simulated CO<sub>2</sub> (trend plus cycle) and observations. The observations are from the March-April and October-November deployments of the Airborne Southern Hemisphere Ozone Experiment / Measurements for Assessing the Effects of Stratospheric Aircraft (ASHOE/MAESA) campaign, when the ER2 made ascents and descents at various latitudes between 70°S and 60°N. Although there are differences between model and observations, the overall variations with altitude, latitude, and season are similar. In March-April, CO<sub>2</sub> decreases monotonically with altitude (for  $\theta > 350$  K) at all latitudes, and the decrease is more rapid in midlatitudes than within the tropics. In October-November the CO<sub>2</sub> profiles in the tropics and low latitudes have a maximum between 350 K and 450 K, with the altitude of the maximum varying with latitude. The occurrence of a maximum in the October-November profiles is due to vertical propagation in the tropics of the maximum in the CO<sub>2</sub> annual cycle in air that entered the tropical stratosphere several months earlier (with quasi-horizontal transport polewards to the extratropics); see Figure 12.

The maximum in the October-November tropical profile is more pronounced in the observations than in the model. To test whether this is due solely to an over attenuation of the signal in the troposphere, or to over attenuation within the stratosphere as well, we have formed CO<sub>2</sub> distributions in which the amplitude of the cycle component has been increased by a constant scaling factor. Figure 16a compares the model tropical profiles in early November when the amplitude of the cycle (shown alone in Figure 16b) has been multiplied by 1, 2, and 3. With the amplitude of the cycle increased by a factor of 2, the tropopause value is larger than that observed, but the stratospheric peak in the CO<sub>2</sub> profile is still smaller than observed. Thus the differences between model and observed CO<sub>2</sub> can not be entirely explained by deficiencies within the model troposphere. The CO<sub>2</sub> cycle is attenuated too rapidly within the model stratosphere, suggesting the influence of midlatitude air on the total CO<sub>2</sub> profile is larger in the model than in the atmosphere or that the model's vertical diffusion is too large or both.

Possibly important for interpretation of observations, the maximum in the modeled November tropical profile of the annual cycle taken alone (Figure 16b) is at a higher altitude than the maximum in the modeled total CO<sub>2</sub> profile (trend plus cycle, Figure 16a) by 40 to 50 K (about 1.3 km). In March/April, a minimum appears in the modeled annual cycle (Figure 16d) but does not appear at all in the modeled total CO<sub>2</sub> profile (Figure 16c). This occurs in the model because the fall-off in concentration with altitude due to the trend alone is more rapid than the increase above the minimum from the annual cycle alone. A minimum in the tropical profile of total CO<sub>2</sub> was not observed from the ER2 in late March 1994 (Figure 15) but was observed in February 1996 [Boering *et al.*, 1996]; the lack of a minimum in March may be consistent with these model results or, alternatively, with propagation of the minimum to altitudes above those sampled by the ER2 in the tropics [Boering *et al.*, 1996]. In both the atmosphere and the model, the degree to which the altitudes of the minima and maxima in the CO<sub>2</sub> annual cycle are displaced from the extrema in the total CO<sub>2</sub> profiles depends on attenuation of the annual cycle relative to the mean fall off of CO<sub>2</sub> with altitude. Thus it may be important to remove the mean fall off in CO<sub>2</sub> mixing ratios (the CO<sub>2</sub> vertical profile averaged over a year or mean age from SF<sub>6</sub> profiles), when more data are available, in order to extract transport rates from the phase lag of the propagation of the CO<sub>2</sub> annual cycle. For example, the model results suggest that the maximum in the total CO<sub>2</sub> profile propagates from 340 K (15.6 km) in early July to 430 K (18.6 km) in early October, while the maximum of the cycle alone reaches 470 K (20 km) by the same time. The phase velocity of the propagating signal derived from the total profile would be a 40% overestimate. In reality, the phase propagation of the cycle and the motion of the CO<sub>2</sub> profile maxima are likely closer, as the cycle amplitude is significantly less attenuated than the model predicts.

## Conclusions

We have used a three-dimensional transport model to simulate the distribution over a year of CH<sub>4</sub>, N<sub>2</sub>O, O<sub>3</sub>, SF<sub>6</sub>, and CO<sub>2</sub> in the stratosphere. The off-line nature of CTMs introduces a degree of approximation because the archived wind data set must be either averaged or subsampled in time to be of manageable size, and all relevant data may not have been archived. We have explored the impact of these approximations by comparing a series of off-line simulations of CH<sub>4</sub> and N<sub>2</sub>O with the resulting fields computed on-line by the GCM. The stratospheric distributions from the off-line simulations vary with the degree of time averaging of the driving data and with the source of the vertical winds, but not with the inclusion of subgrid scale parameterized mixing in the troposphere. The vertical

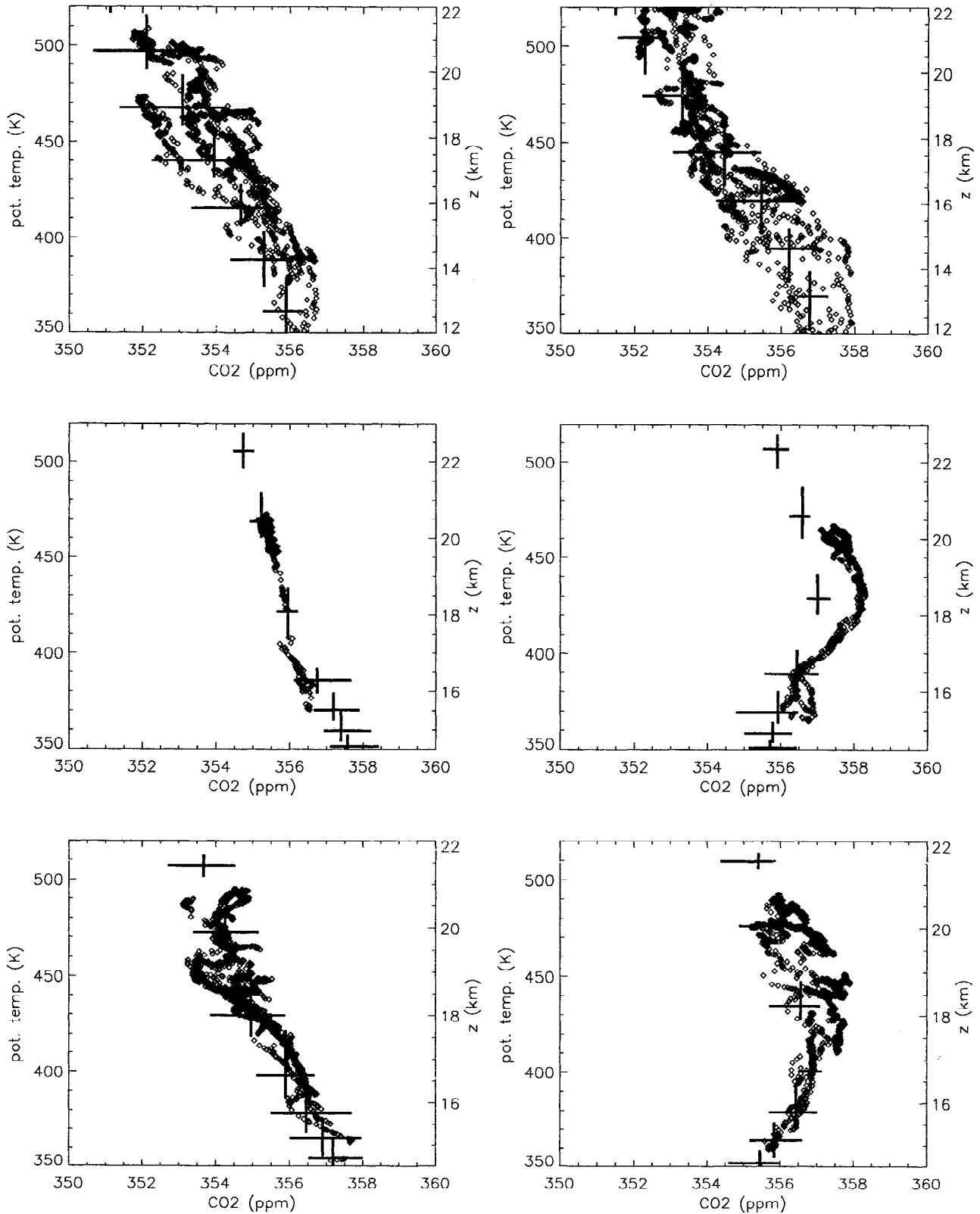


**Figure 15.** Vertical profiles of CO<sub>2</sub> versus potential temperature  $\theta$  in (left) March-April 1994 and (right) October-November 1994 at three latitude bins; (top) 40°-50°S, (middle) 5°S-5°N, (bottom) 10°-20°N. The approximate height, in kilometers, is also shown. The symbols are measurements from the ASHOE/MAESA campaign. The crosses represent the model values at each model level, for March 20 and November 4, respectively; the horizontal (vertical) line shows the range of CO<sub>2</sub> ( $\theta$ ) within each latitude bin, for all longitudes, at given model level.

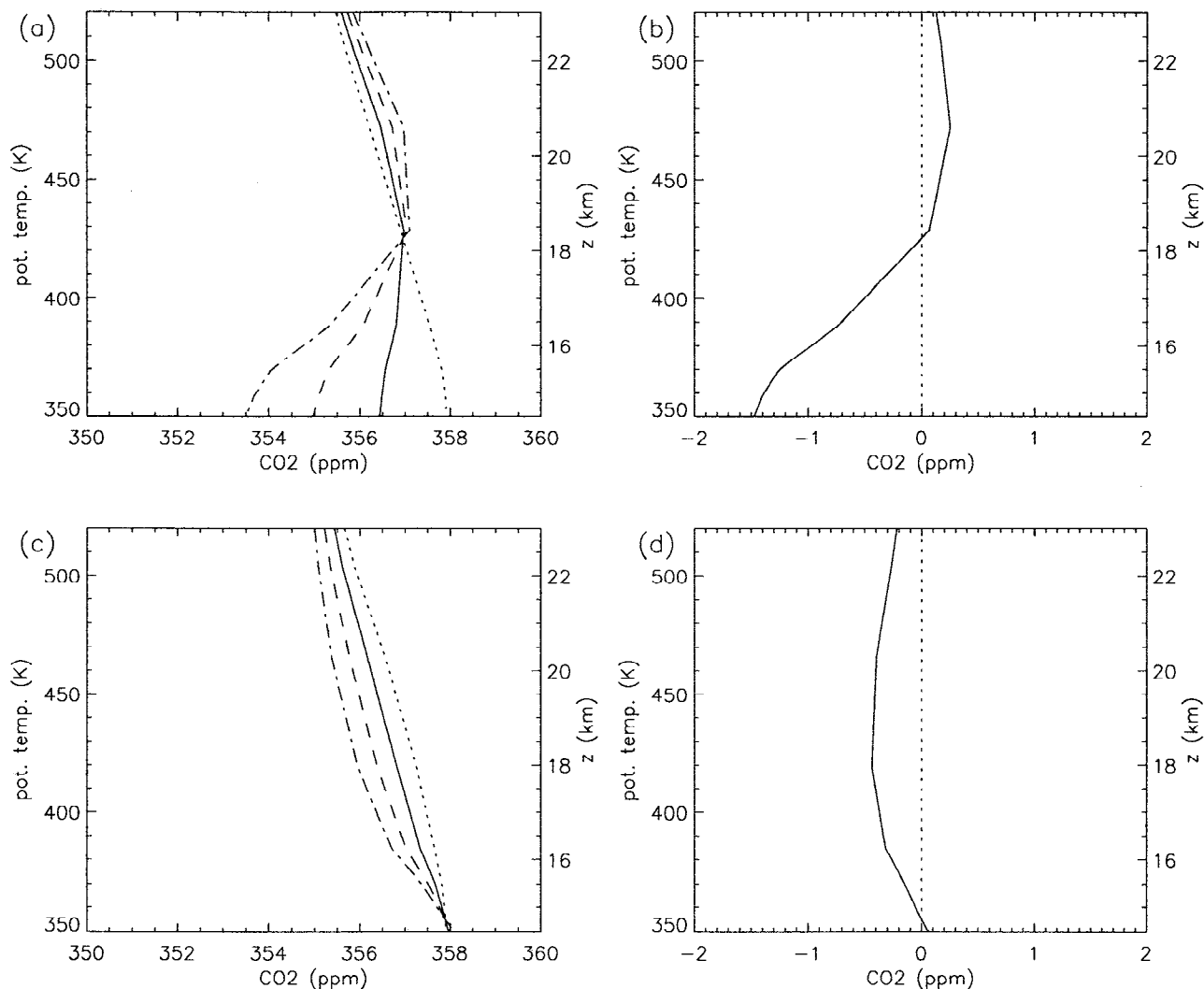


**Figure 16.** Vertical tropical profiles of zonally averaged  $\text{CO}_2$  of the CTM at (a, b) November 4 and (c, d) March 20. Figures 16a and 16c display the response to the  $\text{CO}_2$  trend alone (dotted), total  $\text{CO}_2$  (trend plus cycle) (solid), total  $\text{CO}_2$  with the cycle amplitude multiplied by 2 (dashed), and by 3 (dot-dashed). Figures 16b and 16d display the response to the annual cycle alone.

gradients of the tracers increase as the time averaging of the driving winds used in the off-line simulations is increased, consistent with the fact that averaging of the winds removes transients that can transport tracer [e.g., *Rasch et al.*, 1994]. A surprising, and unexplained, result is that the difference between off-line simulations using 6-hourly averaged driving data and the on-line distributions is comparable to that for simulations using 24-hourly averaged data.

Off-line simulations using driving data subsampled in time have also been performed. These show significant differences from the on-line simulations, even for simulations of only a few months. This indicates that for accurate multiyear off-line simulations using instantaneous fields, such as data from meteorological assimilation systems, the driving data are required at least 6 hourly.

The differences in the zonal mean distributions of  $\text{CH}_4$  and  $\text{N}_2\text{O}$  between off-line simulations using av-

eraged winds and the on-line simulations are substantially smaller than the differences of either simulation from observations. This gives us confidence that we may meaningfully use the off-line model for further studies, deducing aspects of transport as computed by the GCM itself. However, larger on-line/off-line differences may occur for simulations of tracers that do not have significant losses in the upper stratosphere, for example,  $\text{SF}_6$ , as transport differences will not be suppressed by the chemical loss.

The CTM-simulated fields generally agree well with both satellite and aircraft observations. The long lived tracers  $\text{CH}_4$  and  $\text{N}_2\text{O}$  show regions of sharp latitudinal gradients in the lower stratosphere separating the tropics from the extratropics and the midlatitude surf zone from the high-latitude winter vortex, all features present in the HALOE/CLAES climatology of  $\text{CH}_4$ . Some discrepancies exist, including a general underestimation of  $\text{CH}_4$  in the upper stratosphere. The modeled

O<sub>3</sub> fields also shows overall agreement with satellite-based climatology (UARS MLS and HALOE as well as SAGE), but there are some discrepancies, such as a height of peak mixing ratio 2 to 5 km too low.

The mean age deduced from our SF<sub>6</sub> simulation is much older than predictions made by other models [Hall and Prather, 1993; ?]; for example, the mean age in the wintertime polar upper stratosphere of our simulation is around 10 years, compared with around 5 years in other models. These older values of mean age agree better with estimates of mean age from aircraft and balloon measurements of SF<sub>6</sub> and CO<sub>2</sub>, although the simulated values in high latitudes are still younger than observed by 1 to 2 years. Also, balloon observations show a region of nearly zero vertical gradient starting above the lower stratosphere, a feature only weakly reproduced in this model.

The annual cycle component of CO<sub>2</sub> represents model transport information supplementing the mean age. In our CO<sub>2</sub> simulation the cycle is too rapidly attenuated as it propagates vertically through the lower tropical stratosphere. Mote *et al.* [1995] made a similar observation in their MACCM2 modeling study of H<sub>2</sub>O. The smallness of the amplitude implies either an insufficient degree of isolation of the model's tropical region, or too much diffusion in the vertical direction, or both. If vertical diffusion in the model is too large, it is likely caused by too coarse a vertical resolution.

Comparison to observations [Boering *et al.*, 1996] shows our CO<sub>2</sub> annual cycle at the tropical tropopause to be both too weak and lagging in phase by about 1 month. Preliminary studies indicate that the amplitude and phase of the CO<sub>2</sub> annual cycle, but not the CH<sub>4</sub> or N<sub>2</sub>O distributions, are sensitive to the inclusion of subgrid scale parameterizations. Thus observations of upper tropospheric CO<sub>2</sub> cycles [Nakazawa *et al.*, 1991; Matsueda and Inoue, 1996] will help to establish appropriate subgrid scale parameterizations for CTMs.

We have shown that the CTM driven by MACCM2 winds produces realistic distributions of long lived tracers over an annual cycle. We are presently examining the correlations among the various tracers, with an eye to determining what departures from the universality of tracer-tracer correlation curves tell us about degrees of isolation of both the tropics and the polar vortex from midlatitudes. We also plan to examine what departures from tracer-tracer correlation curves universality say about the relative rates of quasi-horizontal mixing and high-latitude descent in the lower stratosphere.

**Acknowledgments.** We thank Dennis Joseph, Brian Eaton, and Pawel Smoikiewicz for providing us archived MACCM2 winds, Jochen Harnisch and Manfred Maiss for providing their balloon measurements of SF<sub>6</sub>, and Rachel Law for development work on the CTM. Rachel Law, Ian Plumb, and Keith Ryan provided helpful comments on an earlier version of the manuscript. This research was supported through the Australian Government Cooperative Research Centre Program.

## References

- Bacmeister, J. T., D. E. Siskind, M. E. Summers, R. R. Conway, and S. Zasadil, Age-of-air in the stratosphere and mesosphere using a zonally averaged, chemical-dynamical model (abstract), *EOS Trans. AGU*, **76**, 130, 1995.
- Bischof, W., R. Borchers, P. Fabian, and B. C. Kruger, Increased concentration and vertical distribution of carbon dioxide in the stratosphere, *Nature*, **316**, 708–710, 1985.
- Boering, K. A., S. C. Wofsy, B. C. Daube, H. R. Schneider, M. Loewenstein, and J. R. Podolske, Stratospheric transport rates and mean age distribution derived from observations of atmospheric CO<sub>2</sub> and N<sub>2</sub>O, *Science*, **274**, 1340–1343, 1996.
- Boville, B. A., Middle atmosphere version of the CCM2 (MACCM2): Annual cycle and interannual variability, *J. Geophys. Res.*, **100**, 9017–9039, 1995.
- Boville, B. A., J. R. Holton, and P. W. Mote, Simulation of the Pinatubo aerosol cloud in a general circulation model, *Geophys. Res. Lett.*, **18**, 2281–2284, 1991.
- Brasseur, G., and S. Solomon, *Aeronomy of the Middle Atmosphere*, D. Reidel, Norwell, Mass., 1984.
- Chipperfield, M. P., D. Cariolle, and P. Simon, A 3D transport model study of chlorine activation during EASOE, *Geophys. Res. Lett.*, **21**, 1467–1470, 1994.
- Conway, T. J., P. P. Tans, L. S. Waterman, K. W. Thoning, D. R. Kitzis, K. A. Masarie, and N. Zhang, Evidence for interannual variability of the carbon cycle from the National Oceanic and Atmospheric Administration/Climate Monitoring and Diagnostics Laboratory Global Air Sampling Network, *J. Geophys. Res.*, **99**, 22831–22855, 1994.
- Conway, T. J., L. S. Waterman, K. W. Thoning, K. A. Masarie, and R. H. Gammon, Atmospheric carbon dioxide measurements in the remote global troposphere, *Tellus*, **40B**, 81–115, 1988.
- Daniel, J. S., S. M. Schauffler, W. A. Pollock, S. Solomon, A. Weaver, L. E. Heidt, R. R. Garcia, E. L. Atlas, and J. F. Vedder, On the age of stratospheric air and inorganics chlorine and bromine release, *J. Geophys. Res.*, **101**, 16757–16770, 1996.
- Douglass, A. R., R. B. Rood, J. W. Waters, L. Froidevaux, W. Read, L. Elson, M. A. Geller, Y. Chi, M. C. Cerniglia, and S. Steenrod, A 3D simulation of the early winter distribution of reactive chlorine in the north polar vortex, *Geophys. Res. Lett.*, **20**, 1271–1274, 1993.
- Douglass, A. R., C. J. Weaver, R. B. Rood, and L. C. Coy, A three-dimensional simulation of the ozone annual cycle using winds from a data assimilation system, *J. Geophys. Res.*, **101**, 1463–1474, 1996.
- Eckman, R. S., W. L. Grose, R. E. Turner, W. T. Blackshear, J. M. Russell, L. Froidevaux, J. W. Waters, J. B. Kumer, and A. E. Roche, Stratospheric trace constituents simulated by a three-dimensional general circulation model: Comparison with UARS data, *J. Geophys. Res.*, **100**, 13951–13966, 1995.
- Elkins, J. W., et al., Airborne gas chromatograph for in situ measurements of long-lived species in the upper troposphere and lower stratosphere, *Geophys. Res. Lett.*, **23**, 347–350, 1996.
- Garcia, R. R., and B. A. Boville, Downward control of the mean meridional circulation and temperature distribution of the polar winter stratosphere, *J. Atmos. Sci.*, **51**, 2238–2245, 1994.
- Garcia, R. R., and S. Solomon, A numerical model of the zonally averaged dynamical and chemical structure of the middle atmosphere, *J. Geophys. Res.*, **88**, 1379–1400, 1983.
- Geller, L. S., J. W. Elkins, R. C. Myers, J. M. Lobert, A. D. Clarke, D. H. Hurst, and J. H. Butler, Tropospheric SF<sub>6</sub>: Observed latitudinal distribution and trends, derived

- emissions, and interhemispheric exchange time, *Geophys. Res. Lett.*, *24*, 675–678, 1997.
- Hall, T. M., and R. A. Plumb, Age as a diagnostic of stratospheric transport, *J. Geophys. Res.*, *99*, 1059–1070, 1994.
- Hall, T. M., and M. J. Prather, Simulations of the trend and annual cycle in stratospheric CO<sub>2</sub>, *J. Geophys. Res.*, *98*, 10,573–10,581, 1993.
- Hall, T. M., and M. J. Prather, Seasonal evolutions of N<sub>2</sub>O, O<sub>3</sub>, and CO<sub>2</sub>: Three-dimensional simulations of stratospheric correlations, *J. Geophys. Res.*, *100*, 16699–16720, 1995.
- Hall, T. M., and D. W. Waugh, Timescales for the stratospheric circulation derived from tracers, *J. Geophys. Res.*, *102*, 8991–9001, 1997.
- Harnisch, J., R. Borchers, P. Fabian, and M. Maiss, Tropospheric trends for CF<sub>4</sub> and C<sub>2</sub>F<sub>6</sub> since 1982 derived from SF<sub>6</sub> dated stratospheric air, *Geophys. Res. Lett.*, *23*, 1099–1102, 1996.
- Hartley, D. E., D. L. Williamson, P. J. Rasch, and R. Prinn, Examination of tracer transport in the NCAR CCM2 by comparison of CFCl<sub>3</sub> simulations with ALE/GAGE observations, *J. Geophys. Res.*, *99*, 12855–12896, 1994.
- Heimann, M., C. D. Keeling, and C. J. Tucker, A three-dimensional model of atmospheric CO<sub>2</sub> transport based on observed winds, 3, Seasonal cycle and synoptic time scale variations, in *Aspects of Climate Variability in the Pacific and Western Americas*, pp. 277–303, *Geophys. Monogr. Ser.*, vol. 55, edited by D. H. Peterson, AGU, Washington, D. C., 1989.
- Lefevre, F., G. P. Brasseur, I. Folins, A. K. Smith, and P. Simon, Chemistry of the 1991–1992 stratospheric winter: Three-dimensional model simulations, *J. Geophys. Res.*, *99*, 8183–8195, 1994.
- Mahlman, J. D., H. Levy, and W. J. Moxim, Three-dimensional simulations of stratospheric N<sub>2</sub>O: Predictions for other trace constituents, *J. Geophys. Res.*, *91*, 2687–2707, 1986.
- Maiss, M., L. P. Steele, R. J. Francey, P. J. Fraser, R. L. Langenfelds, N. B. A. Trivett, and I. Levin, Sulfer hexafluoride: A powerful new atmospheric tracer, *Atmos. Environ.*, *30*, 1621–1629, 1996.
- Matsueda, H., and H. Y. Inoue, Measurements of atmospheric CO<sub>2</sub> and CH<sub>4</sub> using a commercial airliner from 1993 to 1994, *Atmos. Environ.*, *30*, 1647–1655, 1996.
- Mote, P. W., K. H. Rosenlof, J. R. Holton, R. S. Harwood, and J. W. Waters, Seasonal variations of water vapor in the tropical lower stratosphere, *Geophys. Res. Lett.*, *22*, 1093–1096, 1995.
- Nakazawa, T., T. Machida, S. Sugawara, S. Murayama, S. Morimoto, G. Hashida, H. Honda, and T. Itoh, Measurements of the stratospheric carbon dioxide concentration over Japan using a balloon-borne cryogenic sampler, *Geophys. Res. Lett.*, *22*, 1229–1232, 1995.
- Nakazawa, T., K. Miyashita, S. Aaki, and M. Tanaka, Temporal and spatial variations of upper tropospheric and lower stratospheric carbon dioxide, *Tellus*, *43B*, 106–117, 1991.
- Patra, P. K., S. Lal, B. H. Subbaraya, C. H. Jackman, and P. Rajaratnam, Observed vertical profile of sulphur hexafluoride (SF<sub>6</sub>) and its atmospheric applications, *Geophys. Res. Lett.*, *102*, 8855–8859, 1997.
- Pollock, W. A., L. E. Heidt, R. A. Lueb, J. F. Vedder, M. J. Mills, and S. Solomon, On the age of stratospheric air and ozone depletion potentials in the polar regions, *J. Geophys. Res.*, *97*, 12993–12999, 1992.
- Prather, M. J., M. B. McElroy, S. C. Wofsy, G. Russell, and D. Rind, Chemistry of the global troposphere: Fluorocarbons as tracers of air motion, *J. Geophys. Res.*, *92*, 6579–6613, 1987.
- Randel, W. J., B. A. Boville, J. C. Gille, P. L. Bailey, S. T. Massie, J. B. Kumer, J. L. Mergenthaler, and A. E. Roche, Simulation of stratospheric N<sub>2</sub>O in the NCAR CCM2: Comparison with CLAES data and global budget analysis, *J. Atmos. Sci.*, *51*, 2834–2845, 1994.
- Randel, W. J., F. Wu, J. M. Russell, and A. E. Roche, Seasonal cycles and QBO variations in stratospheric CH<sub>4</sub> and H<sub>2</sub>O observed in UARS HALOE data, *J. Atmos. Sci.*, in press, 1997.
- Rasch, P. J., B. A. Boville, and G. P. Brasseur, A three-dimensional general circulation model with coupled chemistry for the middle atmosphere, *J. Geophys. Res.*, *100*, 9041–9071, 1995.
- Rasch, P. J., X. Tie, B. A. Boville, and D. L. Williamson, A three-dimensional transport model for the middle atmosphere, *J. Geophys. Res.*, *99*, 999–1017, 1994.
- Rasch, P. J., and D. L. Williamson, On shape-preserving interpolation and semi-Lagrangian transport, *SIAM, J. Sci. Stat. Comput.*, *11*, 656–687, 1990.
- Ravishankara, A. R., S. Solomon, A. A. Turnipseed, and R. F. Warren, Atmospheric lifetimes of long-lived halogenated species, *Science*, *259*, 194–199, 1993.
- Rayner, P. J., and R. M. Law, A comparison of modelled responses to prescribed CO<sub>2</sub> sources, *Coop. Res. Cent. for South. Hemisphere Meteorol. Tech. Rep. 1*, 1996.
- Remsburg, E., and M. J. Prather, The atmospheric effects of stratospheric aircraft: Reports of the 1992 models and measurements workshop, *NASA Ref. Publ.*, *1292*, 1993.
- Rinsland, C. P., M. R. Gunson, M. C. Abrams, L. L. Lowes, R. Zander, and E. Mahieu, ATMOS/ATLAS 1 measurements of sulfur hexafluoride SF<sub>6</sub> in the lower stratosphere and upper troposphere, *J. Geophys. Res.*, *98*, 20491–20494, 1993.
- Rood, R. B., A. R. Douglas, J. Kaye, M. A. Geller, Y. Chi, D. J. Allen, E. M. Larson, E. R. Nash, and J. E. Neilsen, Three-dimensional simulations of wintertime ozone variability in the lower stratosphere, *J. Geophys. Res.*, *96*, 5055–5071, 1991.
- Rood, R. B., J. Kaye, A. R. Douglas, D. J. Allen, S. D. Steenrod, and E. M. Larson, Wintertime nitric acid chemistry: Implications for three-dimensional model calculations, *J. Atmos. Sci.*, *47*, 2696–2709, 1990.
- Sassi, F., R. R. Garcia, and B. A. Boville, The stratopause semiannual oscillation in the NCAR Community Climate Model, *J. Atmos. Sci.*, *50*, 3608–3624, 1993.
- Schmidt, U., and A. Khedim, In situ measurements of carbon dioxide in the winter arctic vortex and at mid-latitudes: An indicator of the age of stratospheric air, *Geophys. Res. Lett.*, *18*, 763–766, 1991.
- Stolarski, R. S., et al., 1995 Scientific Assessment of the Atmospheric Effects of Stratospheric Aircraft, *NASA Ref. Pub. 1381*, 1995.
- Strahan, S. E., and J. D. Mahlman, Evaluation of the SKYHI general circulation model using aircraft N<sub>2</sub>O measurements, 1 Polar winter stratospheric meteorology and tracer morphology, *J. Geophys. Res.*, *99*, 10305–10318, 1994.
- Williamson, D. L., and P. J. Rasch, Two-dimensional semi-Lagrangian transport with shape preserving interpolation, *Mon. Weather Rev.*, *117*, 102–129, 1989.

K. A. Boering, B. C. Daube, and S. C. Wofsy, Department of Earth and Planetary Sciences, Harvard University, Cambridge, MA 02138. (e-mail: kab@io.harvard.edu; bcd@io.harvard.edu; scw@io.harvard.edu)

B. A. Boville, W. J. Randel, and P. J. Rasch, National Center for Atmospheric Research, P.O. Box 3000, Boulder, CO 80307. (e-mail: boville@ncar.ucar.edu; randel@ncar.ucar.edu; pjr@ncar.ucar.edu)

G. S. Dutton, J. W. Elkins, and C. M. Volk, Climate Monitoring and Diagnostics Laboratory, NOAA, Boulder, CO 80303 (e-mail: gdutton@cmdl.noaa.gov; jelkins@cmdl.noaa.gov; mvolk@cmdl.noaa.gov)

D. W. Fahey, Aeronomy Laboratory, NOAA, Boulder, CO 80303 (e-mail: fahey@al.noaa.gov)

T. M. Hall and D. W. Waugh, Cooperative Research Centre for Southern Hemisphere Meteorology, Monash Univer-

sity, Wellington Rd, Clayton, Vic 3168, Australia (e-mail: hall@vortex.shm.monash.edu.au; waugh@vortex.shm.monash.edu.au)

P. F. Vohralik, CSIRO Divison of Telecommunications and Industrial Physics, Lindfield, New South Wales, Australia (email: vohralik@dap.csiro.au)

(Received January 9, 1997; revised March 7, 1997; accepted March 11, 1997.)